TRANSPORTATION RESEARCH BOARD
NATIONAL RESEARCH COUNCIL

IDEA

Innovations Deserving Exploratory Analysis Project

NATIONAL COOPERATIVE HIGHWAY RESEARCH PROGRAM

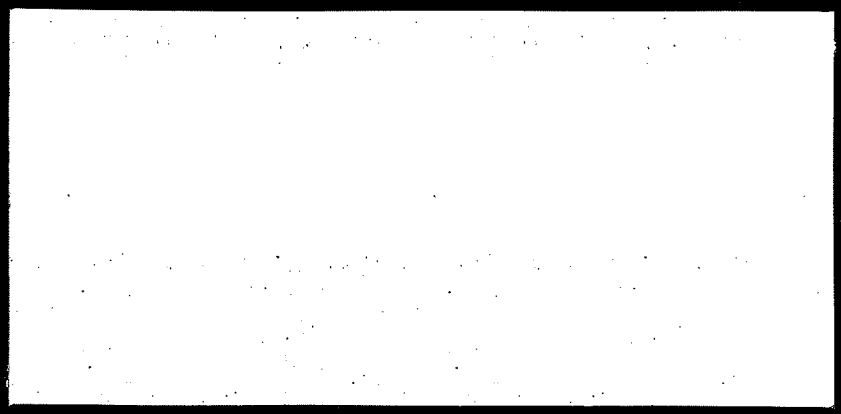

Report of Investigation

IDEA PROJECT FINAL REPORT
Contract NCHRP-96-IDO29

IDEA Program
Transportation Research Board
National Research Council

August 1997

SUPERELASTICITY-BASED REHABILITATION AND POST-TENSIONING OF BRIDGE STRUCTURES

Prepared by:
Parviz Soroushian
Michigan State University
&
Jer-Wen Hsu
DPD, Inc.

INNOVATIONS DESERVING EXPLORATORY ANALYSIS (IDEA) PROGRAMS
MANAGED BY THE TRANSPORTATION RESEARCH BOARD (TRB)

This NCHRP-IDEA investigation was completed as part of the National Cooperative Highway Research Program (NCHRP). The NCHRP-IDEA program is one of the four IDEA programs managed by the Transportation Research Board (TRB) to foster innovations in highway and intermodal surface transportation systems. The other three IDEA program areas are Transit-IDEA, which focuses on products and results for transit practice, in support of the Transit Cooperative Research Program (TCRP), Safety-IDEA, which focuses on motor carrier safety practice, in support of the Federal Motor Carrier Safety Administration and Federal Railroad Administration, and High Speed Rail-IDEA (HSR), which focuses on products and results for high speed rail practice, in support of the Federal Railroad Administration. The four IDEA program areas are integrated to promote the development and testing of nontraditional and innovative concepts, methods, and technologies for surface transportation systems.

For information on the IDEA Program contact IDEA Program, Transportation Research Board, 500 5th Street, N.W., Washington, D.C. 20001 (phone: 202/334-1461, fax: 202/334-3471, http://www.nationalacademies.org/trb/idea)

TABLE OF CONTENTS

EXECUTIVE SUMMARY

The technology discussed here uses superelasticity-based systems for repair and strengthening of bridge structures and also for incorporating unique features for damage control and self-repair into structures. Some key attributes of the system are: (1) efficiency and speed of application; (2) stability and reliability over time under weathering and load effects; (3) damage control under severe load effects; and (4) inherent capability for self-repair. Superelastic alloys are capable of recovering large strains (up to 10%), and can apply large stresses (as high as 700 MPa, 100 ksi) when this strain recovery is constrained. Superelastic alloys also exhibit shape-memory attributes, which can be used advantageously in prestressing applications. Our approach involves repair and strengthening of reinforced concrete structures through post-tensioning with superelastic-based reinforcement. This reinforcement may be in the form of superelastic rods or superelastic fiber reinforced polymer composites. Structures repaired/strengthened with superelastic-based systems also exhibit unique damage control and self-repair capabilities. Our project selected a superelastic alloy with high recoverable strain, recovery stress, elongation capacity and ultimate strength for application to bridge structures. Through a comprehensive experimental work we verified desirable performance of the selected alloy in terms of mechanical characteristics, superelastic attributes, corrosion resistance, and stability under sustained and cyclic loads as well as variable temperatures. We also developed structural design procedures for repair and strengthening of reinforced concrete beams through post-tensioning with superelasticity-based systems. These design techniques accounted for the repair, strengthening and self-repair features of the technology. We then conducted an experimental work which successfully demonstrated the repair, strengthening and self-repair functions of superelastic rods in post-tensioning application to a damaged reinforced concrete beam. We also experimentally verified the strengthening and self-repair features of superelastic fiber reinforced composite sheets bonded onto concrete surfaces. Our comparative cost analysis in the case of a reinforced concrete bridge pier cap in need of shear strengthening indicated that the superelasticity-based approach yielded major cost saving and substantial reduction in the required bridge closure duration when compared with a conventional approach involving post-tensioning with steel strands. These cost and time savings would be accompanied with improved levels of durability and reliability with unique damage control and self-repair attributes.

INTRODUCTION AND OBJECTIVES

INTRODUCTION

The technology discussed here concerns expedient, high-quality and cost-efficient rehabilitation and upgrading of bridges and other structures. The new system can also apply post-tensioning forces in new construction. Our approach takes advantage of the constrained recovery and superelastic behavior of shape-memory alloys for active strengthening and post-tensioning of structural systems and providing them with self-repair capability. The key attributes of our new repair/strengthening technology are: (1) ease and speed of application; (2) stability under weathering and load effects; (3) damage control under severe loading condition; and (4) inherent capability for self-repair.

Shape-memory materials will, after an apparent plastic deformation, return to their original shape when heated; constraint of this shape recovery can generate a considerable force. The same class of materials can be made to exhibit superelasticity at ambient temperature. Superelastic alloys can be strained as much as 10% and still return to their original shape (length) when unloaded. The shape-memory and superelasticity phenomena depend on the occurrence of a specific phase change in the material known as martensitic transformation.[1]

At temperatures below the transformation temperature, shape-memory alloys are martensitic. Heating above the transformation temperature prompts recovery of the austenite (parent) phase. Martensite and austenite phases of the same shape-memory alloy exhibit distinctly different material properties. Figure 1a schematically shows martensite and austenite stress-strain curves. The austenite phase possesses a memory shape which, irrespective of deformations in the martensite phase, would be recovered upon phase transformation. Figure 1b presents the process of free recovery; this is caused, after an apparent plastic deformation in the martensite phase, by phase transformation through heating. Figure 1c shows the generation of force when martensite (low-temperature) strains can not be recovered upon heating due to the presence of constraints against strain recovery.

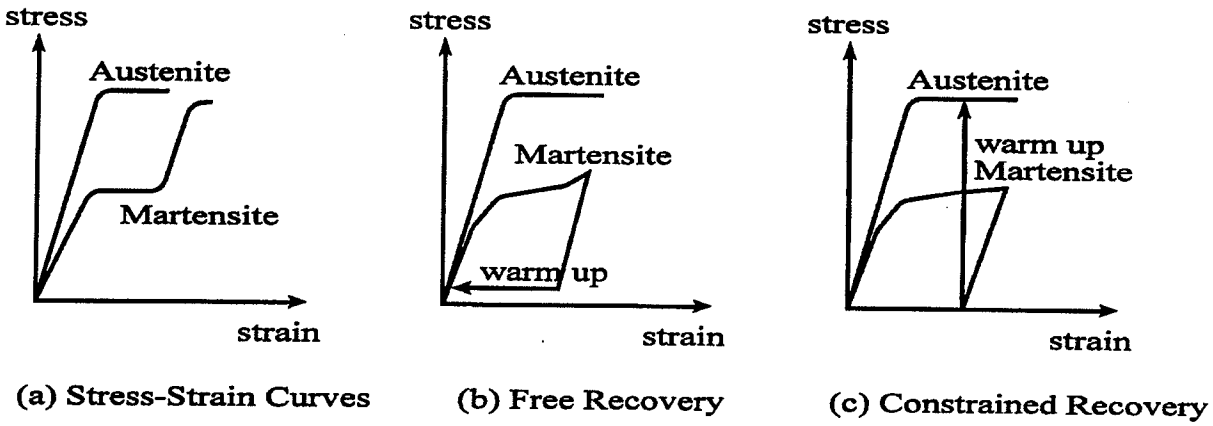

FIGURE 1. Shape-Memory Behavior

Superelasticity (Figure 2) occurs within a temperature range where the shape-memory alloy is austenite but can be transformed to martensite under stress.[2] The parent (austenite) phase would be recovered upon stress removal. The upper plateau in Figure 2 corresponds to the formation of martensite under stress, and the lower plateau represents reversion of the stress-induced martensite upon stress release. Strains up to 10% can be forcefully recovered through this process. The transformation temperatures of shape-memory alloys as well as the superelasticity temperature range and stress plateaus can all be adjusted over a wide range through proper selection of the alloy composition and processing variables.[1]

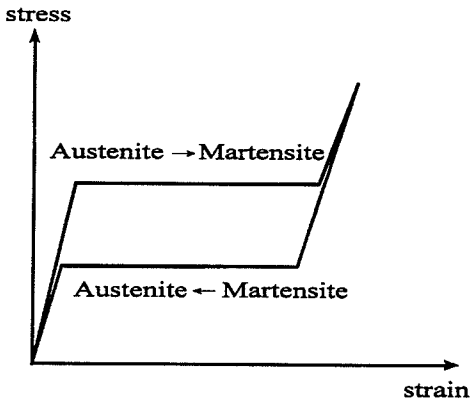

FIGURE 2. Superelastic Behavior

Shape-memory and superelastic alloys based on nickel-titanium (Ni-Ti) have found broad commercial applications. These alloys can be modified by the addition of Cu, Fe, V and Nb to yield characteristics suiting different applications. Other alloys exhibiting superelasticity and shape-memory behavior include copper-based alloys (Cu-Zn-Al and Cu-Al-Ni) and a broad group of iron-based alloys. Today, alloys based on Ni-Ti are the most widely used shape-memory and superelastic alloys, combining pronounced shape-memory effects with high corrosion resistance and a desirable balance of engineering properties.[1] Ni-Ti alloys can recover strains as high as 10% upon transformation to the austenite phase; if constrained, this tendency towards shape recovery can generate stresses as high as 700 MPa (100 ksi). The austenitic elastic modulus of Ni-Ti is close to 80 GPa (12,000 ksi).

Our approach relies on the constrained recovery of superelastic and shape-memory alloys for the rehabilitation and strengthening of existing bridge structures and post-tensioning of new prestressed concrete systems. This approach uses a superelastic rod or a superelastic fiber reinforced polymer matrix composite (Figure 3a). The superelastic system should be engineered to provide a transformation temperature below the ambient temperature and a superelastic temperature range centered around the service (outdoor) temperature of bridge structures, with the alloy remaining austenitic at the lowest anticipated temperature. Figure 3b schematically shows two reinforced concrete beams rehabilitated or reinforced with superelastic rods and superelastic reinforced composite. Both systems in this figure are prestrained. One may use conventionally prestressing techniques for the application of superelasticity-based systems to structures. Also, the forceful recovery phenomenon in shape-memory alloys could be used to facilitate the process. For this purpose, the reinforcement system should be cooled down below transformation temperature, strained at a convenient location, attached to the structure, and then allowed to warm up for the shape recovery process to apply the prestressing force by simply heating the reinforcement system.

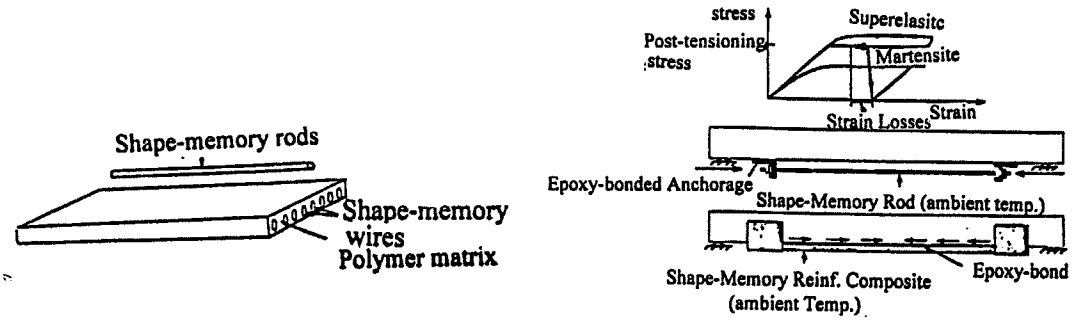

FIGURE 3. Post-Tensioning and Strengthening of Structural Systems

Our approach offers the following unique features in post-tensioning and strengthening of bridge structural systems:

1. Since unloading of the alloy takes place over a plateau with essentially constant stress (Figure 4a), large unloading strains associated with creep, shrinkage, anchorage slip/deformation, elastic deformations, etc. can be accommodated without any loss of the post-tensioning force. This facilitates the application of post-tensioning to situations (e.g. over short lengths) where excess losses preclude the use of traditional post-tensioning techniques.
2. The system can be applied quite rapidly and requires minimal on-site equipment and personnel, minimizing the duration of road closure and the associated costs. Its practical immunity to the loss of prestressing force allows the use of bonded anchorages which are quite simple and expedient but their large creep deformations complicate the use of conventional prestressing techniques.
3. Excess overloads (e.g. over-capacity trucks) and strong energy inputs (e.g. severe earthquakes) can be absorbed by the superelastic-based system which stretches along the loading (upper) stress plateau (Figure 4b) without strain localization, and thus absorbs substantial energy and effectively controls the damage caused by such destructive effects.
4. Upon removal of the damaging effect (e.g. after a severe earthquake), the forceful shape recovery of the alloy along the unloading plateau (Figure 4c) generates corrective motions and forces which provide the structure with an inherent intelligence for self-repair.
5. The high ultimate strength and strain-hardening modulus of superelastic alloys provide added structural capacity under excess loads. The high corrosion resistance of Ni-Ti and some other superelastic alloys also makes the superelasticity-based systems reliable over long service lives of bridge structures in harsh climates.

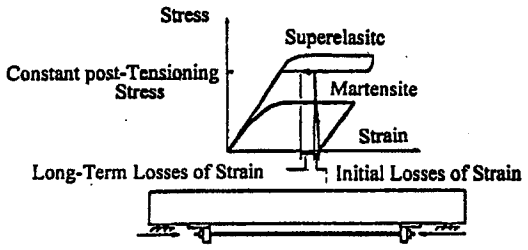

Figure 4 A

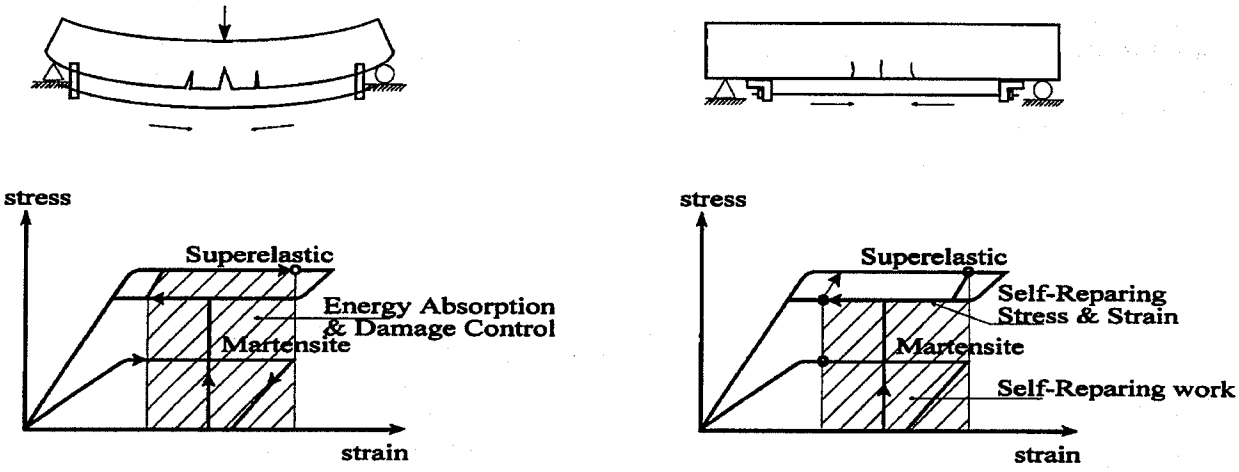

(a) Stress-Strain Curves

(b) Stress-Strain Curves

Figure 4 B

Figure 4 C

FIGURE 4. Some Unique Features of the Technology

OBJECTIVES

The main thrust of this project was to determine the technical feasibility and economic viability of superelastic-based repair/strengthening systems. The project successfully accomplished this goal through achieving the following objectives.

1. Select the composition and processing condition of superelastic alloy suiting repair/strengthening of bridge structures.
2. Develop design techniques for repair/strengthening of reinforced concrete structures with superelasticity-based systems.
3. Experimentally verify the technology.
4. Determine the competitive cost position of superelastic-based repair and strengthening systems.

SELECTION OF THE ALLOY COMPOSITION AND PROCESSING CONDITION

BACKGROUND

Our project focuses on alloys based on nickel-titanium (Ni-Ti). Copper- and iron-based alloys are also available and offer attractive technical characteristics at low cost for our targeted application. Alloys based on Ni-Ti, however, have been subject of more comprehensive research, development and commercial use in the past and thus currently provide a better choice for of our work on the development and validation of the technology.

Binary Ni-Ti alloys offer relatively low unloading plateau stress levels and limited superelasticity temperature range.[3] In order to raise the unloading stress plateau and broaden the superelasticity temperature range, the common method is to dope the alloy with chromium, aluminum, iron or cobalt. This practice lowers the transformation temperature (i.e. broadens the superelasticity temperature range) and allows effective use of cold working followed by annealing in order to raise the plateau stress levels.[2]

Superelastic alloys can be processed to provide diverse cross sectional dimensions and mechanical properties through a combination of cold working (drawing) and annealing. A typical reduction in area between anneals during cold working is about 30% and can be as high as 65%. Interpass annealing is carried out at temperatures between 400 and 800°C usually in air. Ni-Ti wires can be cold worked to diameters as small as 0.075 mm. Upon cold working, Ni-Ti alloys do not show superelastic behavior (see Figure 5). In order to achieve maximum superelasticity, the material has to be heat treated; Figure 5 shows the effects of annealing at two different temperatures on stress-strain behavior. The cold working and annealing conditions strongly influence the stress-strain behavior of superelastic alloys. Higher cold working levels as well as smaller anneal temperatures and durations favor higher plateau stress levels and wider superelasticity temperature ranges.

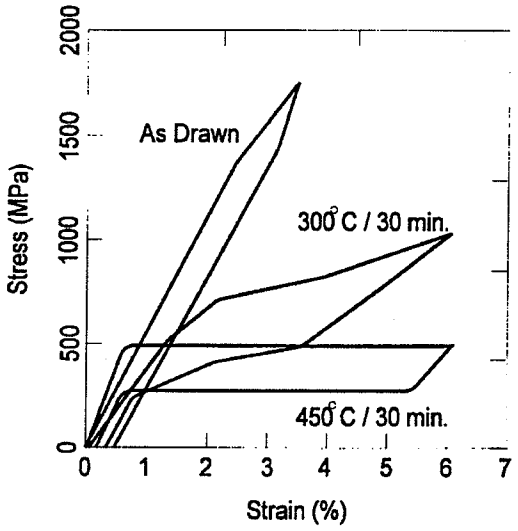

FIGURE 5. Tensile Behavior of an Ni-Ti Alloy After Different Annealing Conditions[1]

THE SELECTION PROCESS

We targeted the following levels of some key superelastic and mechanical characteristics for the selection of the alloy composition and processing condition:

- Recovery (unloading plateau) stress ≥ 250 MPa
- Recoverable strain ≥ 7%
- Loading plateau stress ≥ 500 MPa
- Ultimate strength ≥ 1000 MPa
- Elongation at failure ≥ 10%

In order to satisfy these requirements, based on our survey of the literature and manufacturers, we selected a chromium-doped Ni-Ti alloy with 55.7 wt.% Ni and 0.2 wt.% Cr; the alloy was cold worked 64% to a diameter of 1.78 mm, and then annealed at three alternative temperatures of 470°C, 510°C and 550°C for 1 minute under a tensile stress of 11 MPa. The resulting cold-drawn and annealed superelastic wires were subjected to the following tests (Figure 6) at 22°C with the purpose of selecting the preferred annealing temperature.

- Cyclic tensile loading-unloading with increasing maximum strains up to 10%
- Uniaxial tensile loading to failure

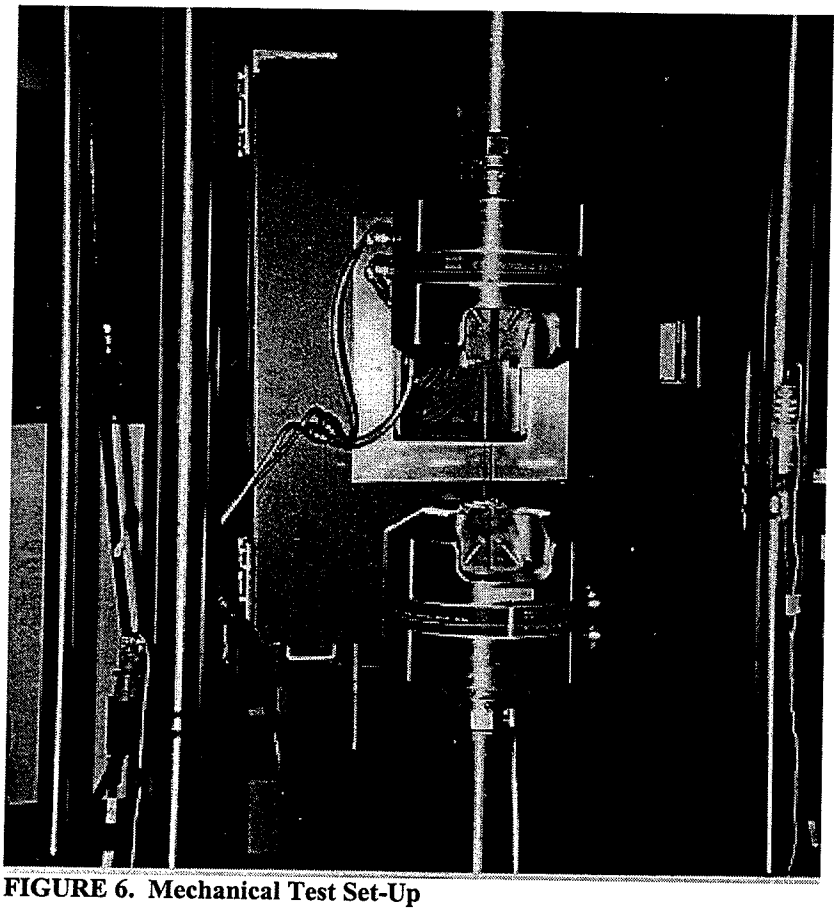

FIGURE 6. Mechanical Test Set-Up

Figures 7a through 7c present the cyclic (tensile loading-unloading) stress-strain behavior of the superelastic wires annealed at different temperatures. Figure 8 compares various aspects of superelastic behavior after annealing at different temperatures. These comparisons suggest that:

- The anneal temperature of 470°C, as compared to 510°C and 550°C, produces inferior superelastic performance with relatively low plateau stresses and high residual strains.
- The superelastic characteristics obtained with 510°C and 550°C anneal temperatures are comparable.
- The ratio of unloading plateau stress to the loading plateau stress is higher with 510°C than with 550°C anneal temperature.
- The ultimate strength of the superelastic wires is somewhat higher with 510°C than with 550°C anneal temperature.

Based on the above findings we selected annealing at 510°C for 1 minute as the preferred condition for maximizing the loading and unloading plateau stress levels and minimizing the permanent strain (i.e. maximizing the recoverable strain).

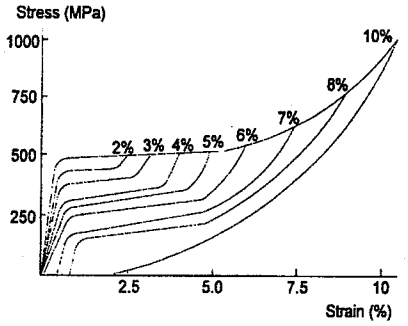

(c) 550° C Anneal Temperatures.

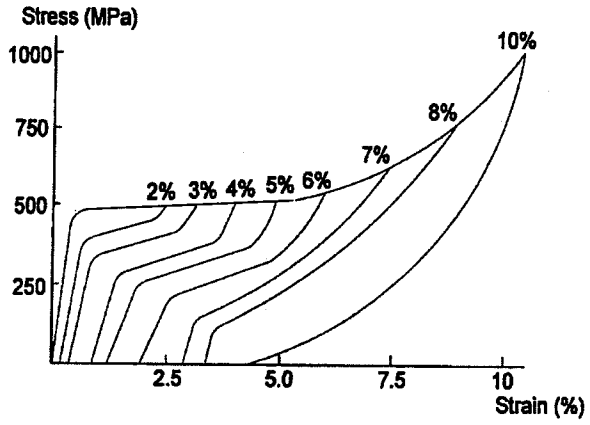

(a) 470° C Anneal Temperatures.

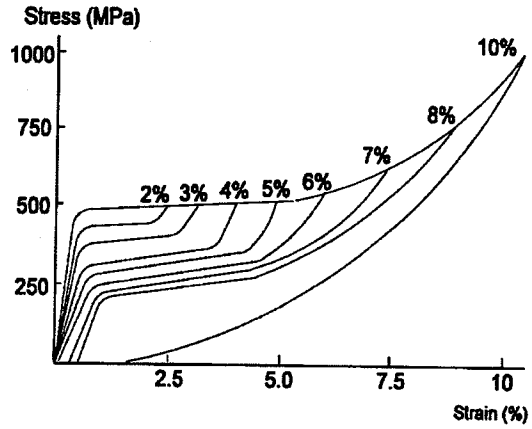

(b) 510° C Anneal Temperatures.

FIGURE 7. Superelastic Stress-Strain Curves After Different Anneal Temperatures

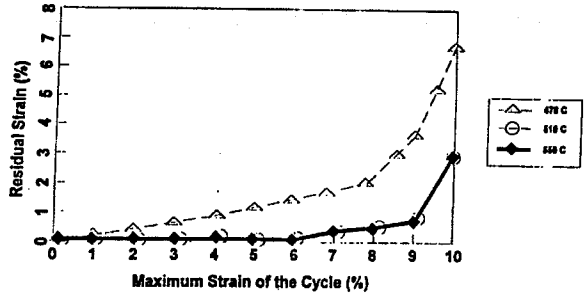

(c) Permanent (Residual) Strain Vs. Maximum Strain of Cycle

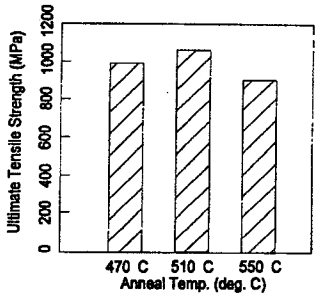

(d) Ultimate Tensile Strength Vs. Anneal Temperature

FIGURE 8. Effects of Anneal Temperature on Superelastic Characteristics

COMPREHENSIVE CHARACTERIZATION OF THE SUPERELASTIC ALLOY

EXPERIMENTAL PROGRAM

We subjected the selected superelastic wire to the following tests in order to fully evaluate it for our targeted application to bridge structures:

- Cyclic tensile loading-unloading with increasing maximum strain levels at different temperatures of 0, 20, 30 and 40°C in order to determine the effectiveness of superelastic reinforcement under different climatic conditions; other temperature ranges should be considered depending on the anticipated service temperatures. The composition and processing conditions of the superelastic alloy should be selected to suit a particular service temperature range.

- Monotonic tensile loading to failure at different temperatures of 0, 20 and 30°C.

- Cyclic tensile loading-partial unloading-reloading to 4%, 2% and 4% strain followed by unloading at 20°C in order to simulate the behavior of pretensioned reinforcement after strain losses when subjected to damaging loads and then load removal where the reinforcement should exert corrective forces.

- Applying a strain of 2% unloading at a temperature of -20°C which is below the transformation temperature of the alloy, constraining the wire ends and allowing it to warm up to the room temperature while monitoring the stresses resulting from the constraint of shape recovery as the alloy temperature rises above its transformation temperature. This loading scheme represents an alternative approach to the application of prestressing forces where the prestrained (and unloaded) cold wires are simply anchored to the structure and allowed to warm up in order to apply the prestressing forces.

- Repeated cyclic loading-unloading to 5% strain in order to assess stability under repeated load cycles.

- Applying a prestrain of 2% to the wire and monitoring the loads over time as the wire is either kept at a constant temperature of 20°C or subjected to temperature cycles of 0°C (72 hours), 20°C (72 hours), 40°C (72 hours) and 20°C (72 hours) in order to assess the relaxation performance of the superelastic reinforcement under climatic effects.

- Corrosion resistance

TEST RESULTS

Cyclic Tensile Stress-Strain Behavior at Different Temperatures

Figure 9 presents the cyclic stress-strain curves at different temperatures. Desirable superelastic characteristics with high plateau stresses and large recoverable strains are observed here at different temperatures. While our selected alloy exhibits a desirable superelasticity temperature range, this range could still be adjusted through refined selection of the alloy composition and processing conditions to suit different climatic conditions.

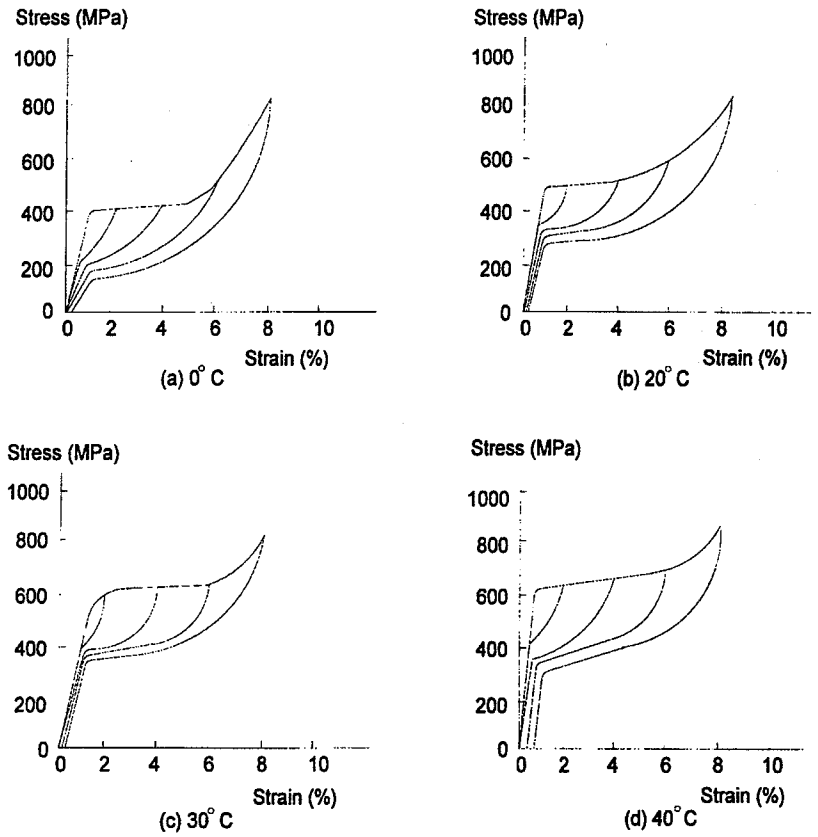

FIGURE 9. Cyclic Stress-Strain Curves at Different Temperatures

Monotonic Tensile Behavior to Failure at Different Temperatures

Figure 10 presents the tensile stress-strain relationships of the superelastic wire at different temperatures. The selected alloy is observed to exhibit desirable levels of strength and ductility at different temperatures. Our test results also confirm that, unlike steel and many other metals, the superelastic reinforcement does not exhibit any "necking" even at relatively large strain levels (within the superelastic strain range) prior to rupture; hence the system exhibits distributed deformations at strains as large as 12%. The superelastic wire can thus absorb substantial energy over its full length as compared to steel and other conventional metals which suffer from an early localization of plastic strains. The distributed nature of large superelastic strains is also attractive in the production of composites from superelastic reinforcement where necking could cause debonding and reduce the possibility for redistribution of damaging effects over a larger volume of the composite system in order to reduce local damage and delay failure.

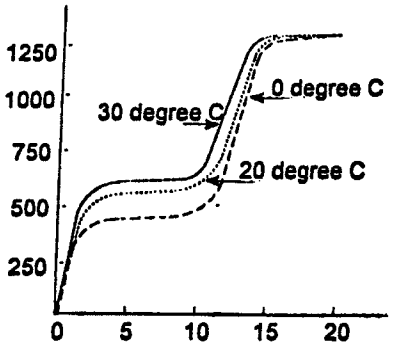

FIGURE 10. Tensile Stress-Strain Relationships at Different Temperatures

Tensile Stress-Strain Behavior Under Partial Load Cycles

Our application of superelastic reinforcement systems to bridge structures involves prestraining of the superelastic reinforcement; this initial prestrain would be partly relaxed over time. Subsequent to that, in case an excessively large load is applied on the structure, the superelastic reinforcement would be again subjected to large strains; upon load removal the superelastic phenomenon will apply corrective forces as the reinforcement recovers over its unloading plateau. In an effort to simulate this behavior we subjected the superelastic wire at a temperature of 20°C to 4% initial strain and then cycled it to 2% and back to 4% strain; finally, we unloaded the wire. The resulting stress-strain relationship (Figure 11) confirms that the unloading plateau stress would be available after this loading history to apply corrective forces to the structure.

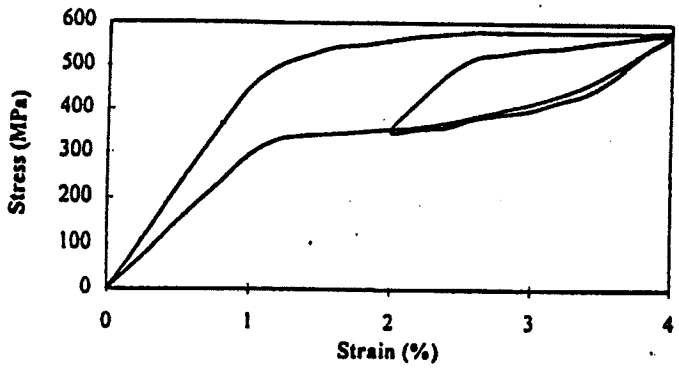

FIGURE 11. Tensile Stress-Strain Relationship Under Partial Load Cycles

Constrained Recovery

Constrained recovery provides a convenient option which could occasionally be used to apply prestressing forces to structures. For this purpose, the superelastic reinforcement is first cooled below its transformation temperature to -20°C where it transforms to the martensite phase (noting that this temperature can be adjusted by the selection of alloy to suit particular service conditions); it is then prestrained (to 2% in this experiment), unloaded, and kept at the low temperature until it is anchored to (and constrained by) the structure. Upon warming to ambient temperature and transformation to the parent austenite phase, the alloy remembers its original length and its tendency to forcefully

recover this length applies prestressing forces to the structure. In this test, with the martensite phase at -20°C we needed 250 MPa tensile stress in order to produce the 2% prestrain in the superelastic wire. Upon warming up to 20°C over a period of 24 hours in constrained condition, the stress required to retain the 2% strain increased to 500 MPa, which is the stress that would have been applied to produce 2% strain in the superelastic wire at 20°C (see Figure 11).

Stability Under Repeated Load Cycles

The superelastic wire exhibited a desirable stability under repeated tensile loading-unloading cycles to 5% maximum strain at 20°C (see Figure 12). This confirms the longevity of the self-repairing capability of the superelastic reinforcement.

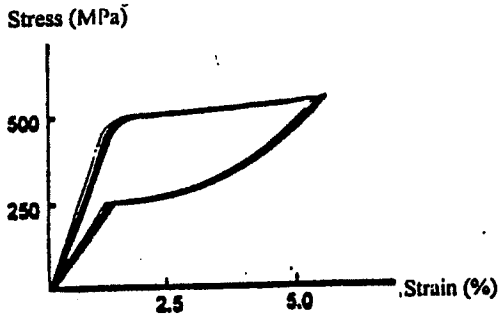

FIGURE 12. Stress-Strain Relationship Under Repeated Load Cycles

Relaxation Characteristics and Corrosion Resistance

The relaxation test set-up is shown in Figure 13. Figure 14 presents results of tensile stress measurement versus time under a constant strain of 2% with temperatures cycling between 0°C, 20°C and 40°C, with the measurements made at 20°C; temperature had a relatively small effect on the stress level in this test. The stress is observed to be stable over time under a sustained level of prestrain.

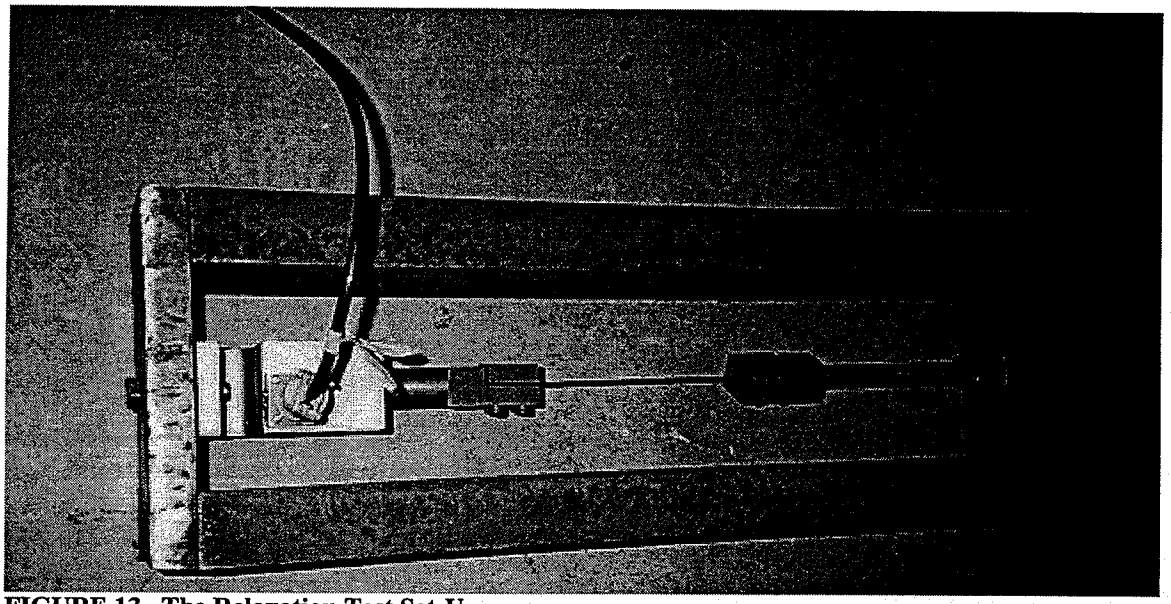

FIGURE 13. The Relaxation Test Set-Up

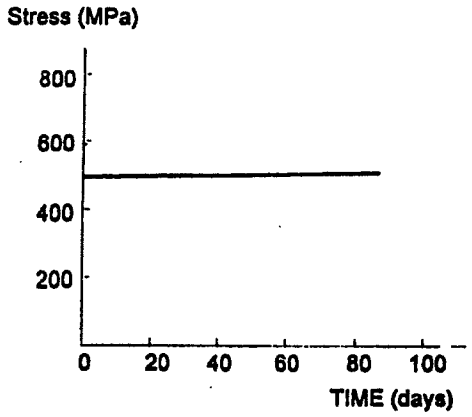

FIGURE 14. Relaxation Test Results Under Cycling Temperatures (test in progress)

Corrosion Resistance

The selected superelastic reinforcement with 1.78 mm diameter as well as stainless steel wires of 1.8 mm diameter were embedded in cylindrical concrete specimens with 75 mm diameter and 150 mm length. These specimens were moist cured for 28 days and then air dried for 7 days prior to immersion in salt water for the measurement of half cell potential (ASTM C 876). The results (Figure 15) indicate that the superelastic wires are even more resistant to corrosion than stainless steel because they exhibit minimal increase in half cell potential. We have recently initiated stress corrosion tests monitoring of which will be continued over time.

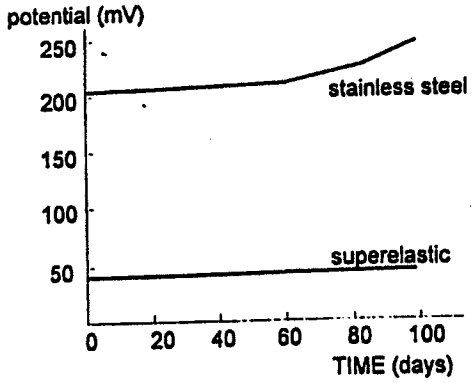

FIGURE 15. Corrosion Resistance Test Results

DEVELOPMENT OF STRUCTURAL DESIGN PROCEDURES

DESIGN OBJECTIVES

We use external post-tensioning with superelastic reinforcement to repair and strengthen reinforced or prestressed concrete structural systems in order to increase their service and ultimate load capacity, and to provide the structure with substantial energy absorption and damage control capability and an inherent self-repairing attribute. End anchorage would be designed following conventional procedures, noting that the practical immunity of superelastic reinforcement

to losses of prestress allows more liberal use of polymeric adhesives with creep deformations that may not be tolerated by conventional prestressing systems.

DESIGN PARAMETERS

Structural design in the context of our approach should lead to decisions on the following parameters: the cross-sectional area, amount of prestrain and geometric configuration of the superelastic reinforcement, and the end anchorage/adhesion of the reinforcement to the concrete structure.

DESIGN CRITERIA

Two sets of design criteria govern post-tensioning with superelastic reinforcement for strengthening and repair: (1) serviceability and strength; and (2) self-repair. The serviceability and strength criteria follow those in conventional prestressing where stress, deflection, crack width and ultimate strength limits have to be satisfied. The self-repair criteria are particular to our approach; here we take advantage of the superelastic phenomenon to build an inherent self-repair capability into the structure, which would be mobilized automatically after a damaging effect such as a severe earthquake, an explosion, or excessive truck loads.

DESIGN METHODOLOGY

Our design methodology seeks to satisfy the two sets of criteria concerning serviceability/strength and for self-repair.

Design for Serviceability and Strength

This aspect of our design employs the conventional prestressing concepts. As compared to prestressing steel (Figure 16a), superelastic reinforcement applies prestressing forces at two constant levels (with limited or no relaxation) associated with its unloading and loading plateaus (Figure 16b). The unloading plateau would be followed over time as concrete experiences creep and shrinkage; the loading plateau would be followed with the application of live loads.

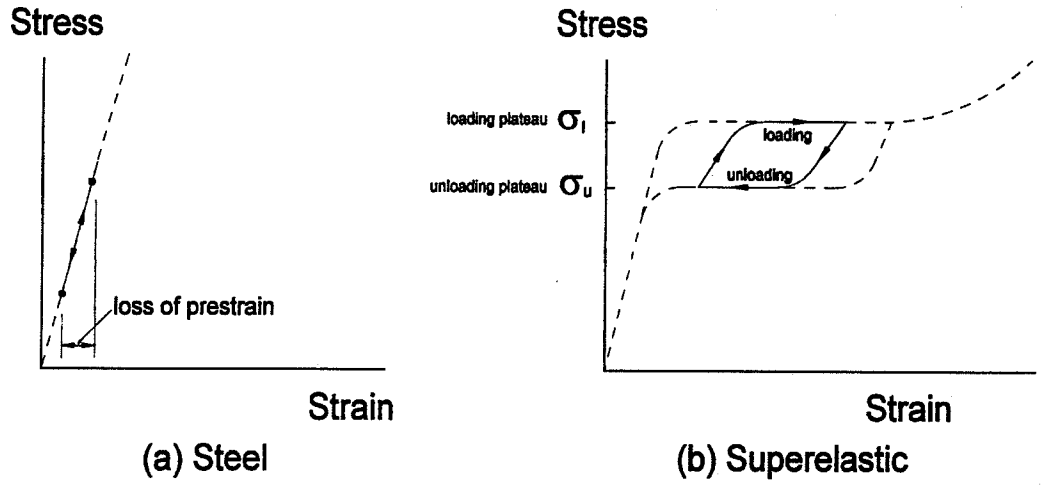

FIGURE 16. Steel Versus Superelastic Stress-Strain Relationships

Design issues relevant to stress limits, flexural strength, deflection limits, allowable crack widths, losses of prestrain, and shear strength for the typical post-tensioning conditions of Figure 17 are discussed below.

Stresses

Initial Stresses Under Dead Load:

$$f_1 = -\frac{P_x}{A_c}\left(1-\frac{e.c_1}{r^2}\right)-\frac{M_o}{S_1}$$

$$f_2 = -\frac{P_x}{A_c}\left(1+\frac{e.c_2}{r^2}\right)+\frac{M_o}{S_2}$$

Stresses Under Full Service Load:

$$f_1 = -(P_x/A_c).(1-e.c_1/r^2) - M_t/S_1$$

$$f_2 = -(P_x/A_c).(1+e.c_2/r^2) + M_t/S_2$$

where: P_x = both P_u and P_l
$P_u = \sigma_u \cdot A_{sp}$
$P_l = \sigma_l \cdot A_{sp}$
A_{sp} = area of the superelastic reinforcement
σ_u = upper plateau stress in superelastic reinforcement (see Figure 16b)
σ_l = lower plateau stress in superelastic reinforcement (see Figure 16b)
A_c = gross cross sectional area
r = radius of gyration of the cross section
M_o = dead load moment
M_t = maximum total moment applied along the length of the reinforcement
e, c_1 and c_2 are shown in Figure 17

The above stress levels should not exceed the following limits which are adapted from prestressed concrete design:

Limit on compressive stresses = $0.45\ f_c'$

Limit on tensile stresses = $6\sqrt{f_c'}$

where: f_c' = compressive strength of concrete (psi)

One may calculate stresses based on cracked section properties (if cracking occurs) in more accurate designs for fatigue, deflection and crack width.[4]

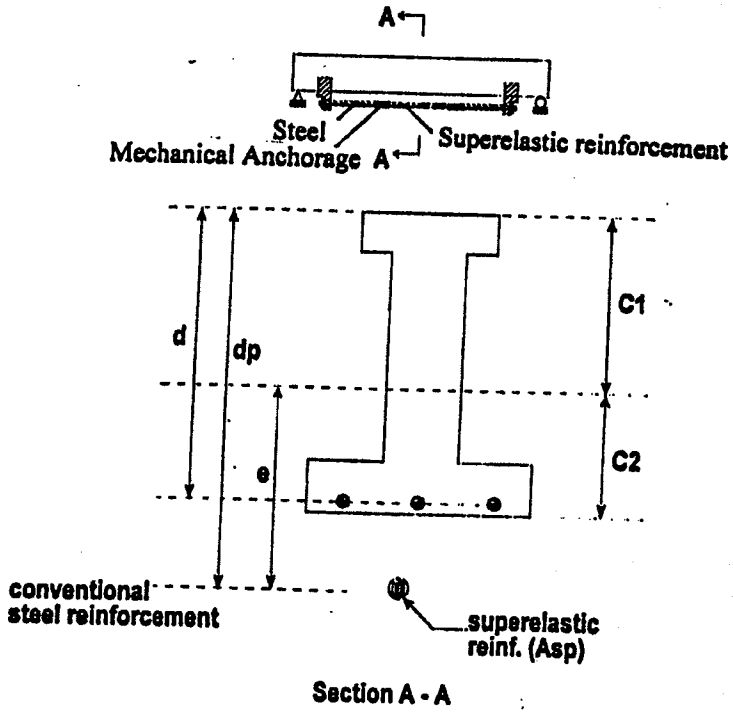

FIGURE 17. External Post-Tensioning with Superelastic Reinforcement

Flexural Strength

The equation for nominal flexural strength (M_n) is as follows:

$$M_n = A_s.f_y.\ (d-a/2) + A_{sp}.\sigma_u.(e+c_1-a/2)$$

where: A_s = area of conventional steel reinforcement
a = depth of compression block (as in conventional design)
d = effective depth (see Figure 17)

The above equation assumes that the strain in superelastic reinforcement at failure does not exceed the maximum strain of the upper plateau; if this is not true, the stress compatibility approach should be used to calculate the strain and stress levels in the superelastic reinforcement to replace σ_u in the above equation.[4] An upper limit on the amount of superelastic reinforcement is defined by the need for the conventional steel to yield at the ultimate load; alternatively, the above equation can be modified to account for the fact that the conventional steel has not yielded.[4]

The nominal flexural strength of the section should be sufficient to resist the maximum factored moment (M_u):

$$M_u \leq \phi.M_n$$

where: ϕ = capacity reduction factor (0.9 in reinforced concrete flexural design per ACI, or 1.0 in prestressed concrete flexural design per AASHTO)

Flexural Crack Widths

We have adapted a traditional reinforced concrete equation for crack width calculation:

$$w=0.076\,\beta.\Delta f_s.\sqrt[3]{dc.A}$$

where: w = maximum crack width in thousandths of inch
$\beta=h_2/h_1$
$A = A_t/(\text{number of bars embedded in concrete, in}^2)$
d_c, h_1, h_2 and A_t are introduced in Figure 18a
Δf_s = the increase in tension beyond the decompression stage:

$$f_{s3} = n_s.[-P_u/A_{ct} + P_u.e^*.(e+c_1-c_1^*)/I_{ct}]$$

where: n_s = ratio of the reinforcing steel to concrete modulus of elasticity
A_{ct} and I_{ct} = the area and moment of inertia of transformed section (Figure 18b)
c_1^* = distance from top to the centroid of the cracked transformed section
$e^* = (M_t-P_u.e)/P_u+c_1-c_1^*$

Bridges are typically subjected to either humidity, deicing chemicals or wetting-drying conditions where the maximum allowable crack widths are 0.3, 0.18 and 0.15 mm, respectively.

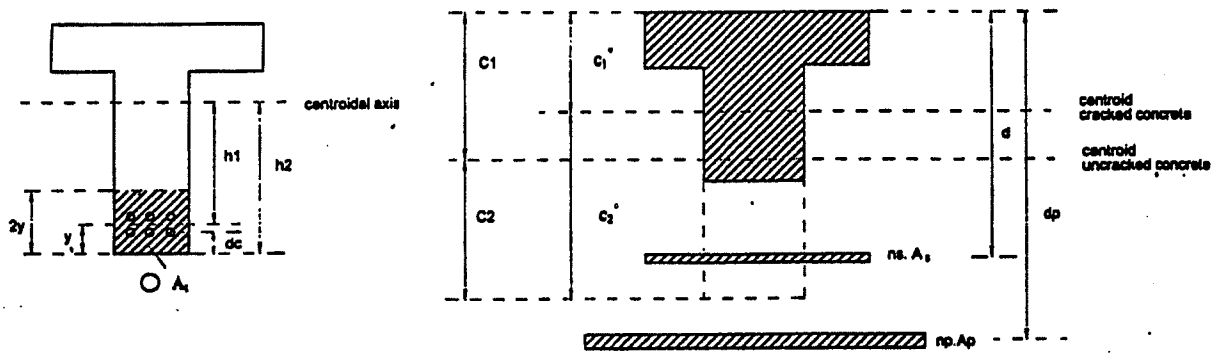

(a) Geometric Attributes **(b) Cracked Transformed Section**

FIGURE 18. Geometric Attributes and Cracked Transformed Section

Deflections

The net deflection due to prestressing is:

$$\Delta = -\Delta(P_{u)} + \Delta_o$$

The long-term deflection due to prestressing is:

$$\Delta = -\Delta(P_l) - [(\Delta(P_u) + \Delta(P_l))/2].C_u$$

Total deflection is:

$$\Delta = -\Delta(P_u) - [(\Delta(P_u) + \Delta(P_l))/2].C_u + (\Delta_o + \Delta_d)(1+C_u) + \Delta_l$$

where: $\Delta(P_u)$ and $\Delta(P_l)$ = deflections under P_u and P_l (upper and lower plateau loads)
Δ_o, Δ_d and Δ_l = deflections under self-weight, dead load and live load, respectively
C_u = creep coefficient (~2.35)

For bridges, the AASHTO specifications require that for simple or continuous spans, the deflection due to live load plus impact should not exceed 1/800 of the span, except on bridges in urban areas used in part by pedestrians, on which the ratio preferably shall be 1/1000. The deflection of cantilever arms due to live load plus impact is limited to 1/300 of the cantilever arm except for the case including pedestrian use, where the ratio preferably shall be 1/375 according to the specification.

Given the significance of live load deflections in bridge structures, a more accurate calculation of live load deflections which accounts for the possibility of cracking in partially prestressed beams seems warranted:

$$\Delta_l = K_l.M_{l1}.L^2/(E_c.I_g) + K_l.(M_l - M_{l1})/(E_c.I_{e,l2})$$

where: K_l = geometric factor for live load
M_l = total live load moment
$M_{l1} = (K_p/K_l).P_u.e - (K_d/K_l).M_d$
K_p and K_d = geometric factors for prestressing force and dead load, respectively
M_d = dead load moment
I_g = gross moment of inertia of the uncracked section
$I_{e,l2} = (M_{cr}/M_{l2})^3.I_g + [1-(M_{cr}/M_{l2})^3].I_{cr}$

Losses of Prestrain and the Required Level of Prestrain

The loss of prestrain in our application is due to anchorage slip, elastic shortening of concrete, creep of concrete, and any remaining shrinkage of concrete. If the element to be repaired/strengthened has suffered excess deflections and cracking, this should be accounted for in the calculation of the "elastic shortening" of concrete unless the post-tensioning forces are applied as the superelastic reinforcement is supported on the structure.

The loss of prestrain due to anchorage slippage ($\Delta\varepsilon_{anc}$) is:

$$\Delta\varepsilon_{anc} = \Delta l/l$$

where: Δl = total anchorage slippage
l = length of the superelastic portion of reinforcement

The loss of prestrain due to creep of concrete ($\Delta\varepsilon_{cp}$) is:

$$\Delta\varepsilon_{cp} = C_u.\ \varepsilon_i.(l_s + l_{sp})/l_{sp}$$

where: $\varepsilon_i = P_i.e.c_1^{\bullet}/(E_c.I_g)$
l_s = the length of steel reinforcement (anchored to the superelastic reinforcement)
l_{sp} = the length of superelastic reinforcement

The loss of prestrain due to shrinkage of concrete ($\Delta\varepsilon_{sh}$) is:

$$\Delta\varepsilon_{sh} = \varepsilon_{sh}.(l_s+l_{sp})/l_{sp}$$

where: ε_{sh} = remaining shrinkage of concrete (if any)

The loss of prestrain due to "elastic shortening" is zero if post-tensioning is performed with the prestressing system supported on the structure. Otherwise, if the shape-memory aspect of the superelastic reinforcement is used to also apply the prestressing force, the loss of prestrain due to "elastic shortening ($\Delta\varepsilon_{sl}$) has two components, one corresponding to the actual elastic shortening after corrective deflections ($\Delta\varepsilon_{sl1}$) , and the other corresponding to the corrective deflections ($\Delta\varepsilon_{sl2}$):

$$\Delta\varepsilon_{sl1} = \{[(-P_i/A_c).(1+e^2/r^2)+M_o.e/I_g]/E_c\}.(l_s+l_{sp})/l_{sp}$$
$$\Delta\varepsilon_{sl2} \approx \Delta_r.e/(K_p.L^2).\ (l_s+l_{sp})/l_{sp}$$

The applied prestrain on the superelastic reinforcement should be such that after all these losses the superelastic reinforcement just retains the strain level needed to stay on the lower plateau of its stress-strain curve (see Figure 19).

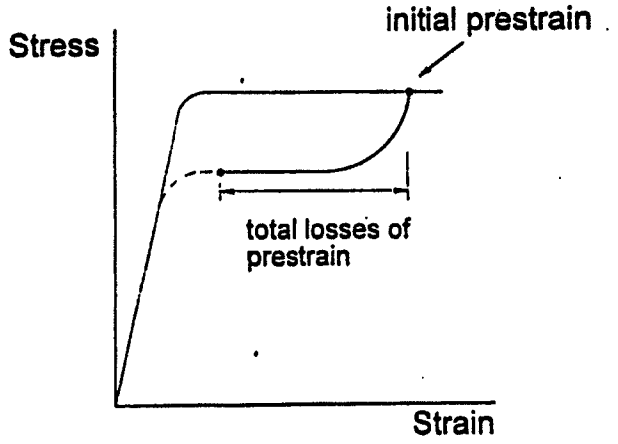

FIGURE 19. The Effect of Losses in Prestrain on Superelastic Reinforcement

Shear Strength

The nominal shear strength of a section (V_n) is the sum of the concrete shear strength (V_c) and the steel shear strength ($V_s = A_v.f_y.d/s$). The concrete shear strength is the smaller of the resistance to flexure-shear cracking (V_{ci}) and to web-shear cracking (V_{cw}), as given below:

$$V_{ci} = 0.6\sqrt{f_c'}\ b_w.d + V_o - (V_i/M_{max}).M_{cr}$$

$$V_{cw} = (3.5\ \sqrt{f_c'}\ +0.3\ f_{cc})b_w.d + V_p$$

where: b_w = width of the rectangular section or the web width of a flanged section
$d \cong 0.8\ h$
V_i & M_{max} = factored shear and moment under superimposed dead and live loads

V_o = unfactored shear due to self-weight
M_{cr} = cracking moment in addition to self-weight
$= (I_g/c_2).(6\sqrt{f_c'} + f_{2p} - f_o)$
f_o = flexural stress in concrete at the bottom face due to self weight
f_{2p} = concrete compressive stress at the bottom face under P_u

Design for Self-Repair

The self-repair capability of the superelastic reinforcement would be activated automatically upon unloading after overloading. Under such overloads the structure would suffer yielding in normal steel, flexural cracking in concrete, and excess deformations. In order to accomplish self-repair, the superelastic reinforcement at its lower plateau stress level must apply sufficient force to produce a counteracting yield moment in the beam and thus close the cracks and correct the deflections. Referring back to Figure 3b, the required area of superelastic reinforcement (A_{sp}) to accomplish this is:

$$A_{sp} = A_s.f_y.(d-c_2^*)/[\sigma_l.(d_p- c_2^*)]$$

At the same time, the application of this counteracting moment should not produce excess stresses at the top section; one may have to strengthen the top section to satisfy this requirement.

The capacity of superelastic reinforcement to absorb damaging energies and strains is determined by the maximum strain of its upper plateau (see Figure 20). This would be another design criterion for the structure should sustain certain damaging energies and still be able to accomplish self-repair. The fact that large superelastic strains do not localize and tend to distribute along the full length of the reinforcement is a major advantage in the absorption of destructive energies and limiting structural damage.

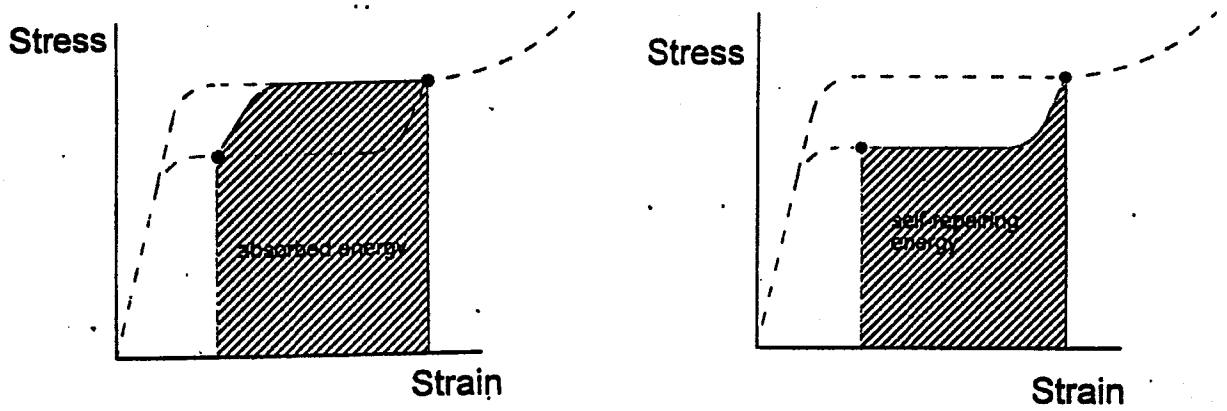

FIGURE 20. Energy Absorption and Self-Repair Under Damaging Effects

A trial and adjustment approach would yield the required levels of eccentricity and superelastic reinforcement area needed to satisfy both the serviceability/strength and self-repair requirements. In case only a fraction of the full length is superelastic and the remaining is steel (to save material costs), the superelastic length fraction of the reinforcement should be selected to accommodate the losses of prestrain and also to provide a minimum strain on the plateaus to absorb damage and accomplish self-repair. For this purpose, one needs to determine the level of destructive energies and to make sure that the reinforcement systems can absorb this energy as superelastic strain energy (underneath the loading superelastic stress-strain curve).

EXPERIMENTAL VERIFICATION OF THE TECHNOLOGY

INTRODUCTION

In order to verify the new repair and strengthening system for concrete structures, we conducted two series of experiments - one using superelastic rods, and the other superelastic fiber reinforced polymer matrix composites. Superelastic rods were used to accomplish repair and strengthening of a reinforced concrete beam in flexure, and also to incorporate self-repair capability into the repaired beam. The composite system was used to strengthen a concrete specimen subjected to tension, and also to provide it with self-repair capability.

THE REINFORCED CONCRETE BEAM

The reinforced concrete beam used for experimental verification of the new repair/strengthening system is shown in Figure 21. This beam was designed with a concrete compressive strength of 28 MPa and a steel yield strength of 415 MPa. The beam is designed for a total service dead load of 3.1 KN and a total service live load of 14.5 KN, with both the dead load and the live load applied at one-third points. The beam provides a nominal flexural strength of 6,382 N.m and a nominal shear strength of 45.3 KN; the total load corresponding to flexural and shear failures are 32.5 KN and 90.6 KN, respectively. Hence, the beam is designed to fail in flexure; Figures 22 and 23 show pictures of the reinforcement in this beam and the beam itself.

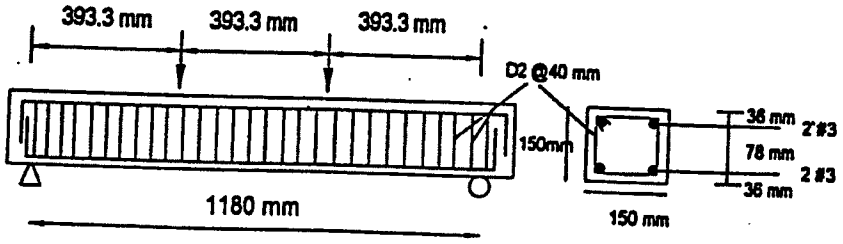

FIGURE 21. The Reinforced Concrete Beam

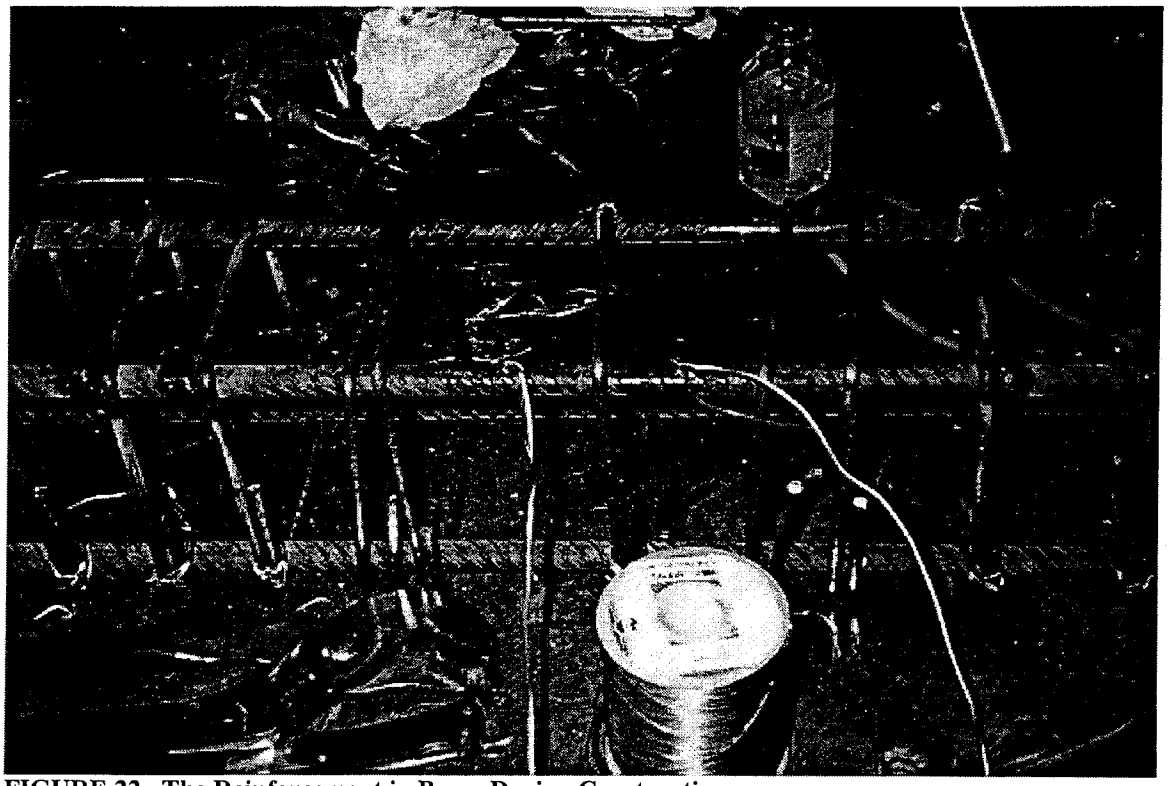

FIGURE 22. The Reinforcement in Beam During Construction

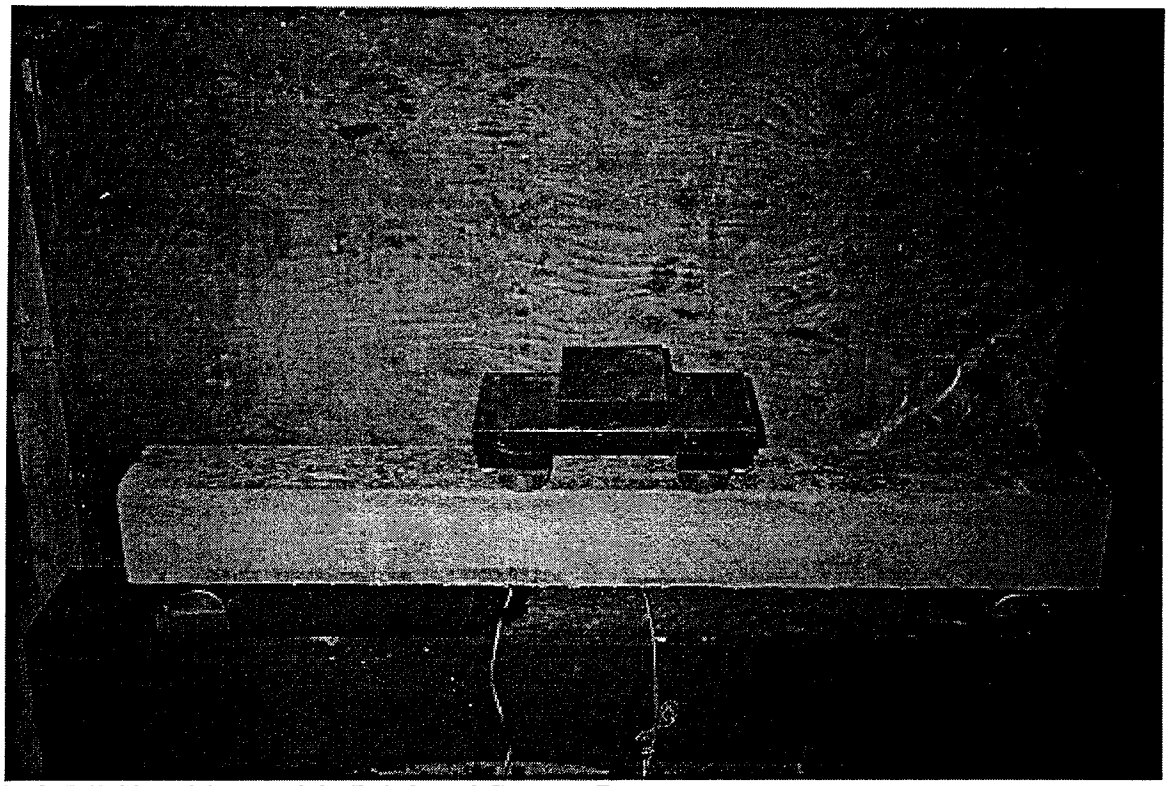

FIGURE 23. A Picture of the Reinforced Concrete Beam

ANALYSIS OF THE UNSTRENGTHENED BEAM

Flexural and Shear Strength

For the original design to be acceptable under the initial loads, the maximum values of moment and shear force under factored loads should not exceed the corresponding nominal strengths multiplied by the capacity reduction factors:

$$M_u < \phi.M_n$$

$$V_u < \phi.V_n$$

In our case:

$$M_u = 5{,}700 \text{ N.m} < \phi.M_n = 0.9\ (6{,}382) = 5{,}744 \text{ N.m} \qquad \surd \text{ o.k.}$$

$$V_u = 14.5 \text{ KN} < \phi.V_n = 0.85\ (45.3) = 38.5 \text{ KN} \qquad \surd \text{ o.k.}$$

Deflection and Crack Width

The total service load of 17.6 KN is applied on the beam at one-third points. This load produces a maximum bending moment of 3,461 N.m which exceeds the cracking bending moment of 1,943 N.m. The effective moment of inertia would thus be somewhere between the gross and the cracked moments of inertia as calculated from the following equation:

$$I_e = I_{cr} + (I_g - I_{cr}) \,.\, (M_{cr}/M_{max})^3$$

With I_{cr} = 1,018 cm^4 and I_g = 4,219 cm^4, one arrives at I_e = 1,584 cm^4 as the effective moment of inertial for our cross section.

The maximum deflection at mid-span can thus be calculated from the following expression:

$$\Delta_{max} = 23\ P.l^3/(1296\ E.I_e)$$

which yields a value of 1.33 mm. This maximum deflection is 0.0011 times the span length, which is within acceptable range under typical conditions (where a maximum deflection of 0.00125 times span length may be tolerated).

We computed maximum crack width using the following expression, which is commonly used in reinforced concrete design:

$$w = 0.076\beta.f_s.\sqrt[3]{d_c.A}$$

This equation yields a crack width of 0.19 mm which is within tolerable range noting that maximum crack widths for exposure conditions involving humidity and deicer salt are 0.3 mm and 0.18 mm, respectively.

DESIGN FOR STRENGTHENING AND REPAIR BY POST-TENSIONING

Strengthening

The purpose of strengthening the beam in this project was to double its capacity for carrying live loads. The total live and dead loads applied at on-third points on the strengthened beam would then be 29 KN and 3.1 KN, respectively. The resulting factored bending moment (11,400 N.m) exceeds the nominal flexural strength of the original section times the capacity reduction factor (5,744 N.m). The maximum bending moment under the new service loads (6,923 N.m) also exceeds the yield strength of the original cross section (6,382 N.m), and thus the deflections and crack widths of the original beam would be excessive if the initial live load is doubled.

Post-tensioning with shape-memory or superelastic reinforcement is the basis of our approach to strengthening of the beam. Figure 24 presents the schematics of the strengthened beam where an eccentricity of 85 mm is specified for the external prestressing (shape-memory or superelastic) reinforcement. We need to analyze the beam in order to determine the magnitude of the prestressing force needed to strengthen the beam for carrying double the initial live load.

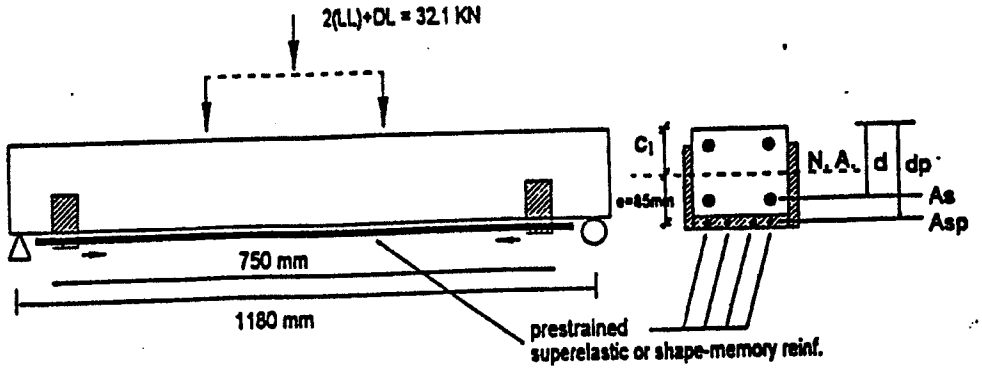

FIGURE 24. Schematics of the Strengthened Beam

Following the prestressed concrete design principles, we used the allowable stress method as the basis to design the corrective (prestressing) force needed for strengthening the beam. The allowable stresses are as follows:

$$\text{in tension:} \quad f_{1,max} = 12\sqrt{f'_c}$$

$$\text{in compression:} \quad f_{2,max} = 0.45 f'_c$$

We can use the following expressions to calculate the tensile and compressive stresses in the beam in terms of the applied prestressing force (P) prior to and after the application of service loads:

Prior to the Application of Service Loads:

$$f_1 = -P/A_c + P.e.c_1 / I_c$$

$$f_2 = -P/A_c - P.e.c_2 / I_c$$

After the Application of Service Loads:

$$f_1 = -P/A_c + P.e.c_1 / I_c - M_{service} / S_1$$

$$f_2 = -P/A_c - P.e.c_2 / I_c + M_{service} / S_2$$

A corrective prestressing force of 55 KN produces tensile and compressive stresses which fall within the acceptable limits. We thus chose 55 KN as the prestressing force to be applied for strengthening of the beam. This force also produces acceptable stress levels at the ends where $M_{service}$ in the above equations approaches zero.

Repair and Strengthening with Superelastic Reinforcement

The superelastic reinforcement we have selected for use in this study provides lower and upper plateau stresses of about 300 and 500 MPa, respectively. For the application of the corrective prestressing force of 55 KN using 1.78-mm diameter superelastic wires, assuming that an average of the upper and lower plateau stresses are applied, we would need a total of 50 wires. We chose the average of upper and lower plateau stresses because initial anchorage slippages would not allow application of the full upper plateau stress.

The initial prestraining of superelastic wires should be sufficient to tolerate strain losses associated with the closure of cracks, elastic deformations, creep, shrinkage and relaxation. Assuming that overloads in the beam have caused yielding of steel and have produced a midspan deflection of 12 mm, crack closure would involve 0.4% strain loss. The sum total of strain losses associated with elastic deformations, creep, shrinkage and relaxation is about 0.2%. Hence, the initial prestrain should be sufficient to tolerate a total loss of 0.6% and still stay on the unloading plateau of the superelastic reinforcement. We have chosen to apply 3% of prestrain in the superelastic reinforcement prior to installation on the beam in order to safely satisfy this requirement.

After strengthening with superelastic reinforcement, the nominal flexural strength of the beam (M_n) can be calculated as follows:

$$M_n = A_s.f_y.(d-a/2) + A_{sp}.\sigma_u.(e+c_1-a/2)$$

where: A_{sp} = area of the superelastic reinforcement
σ_u = upper plateau stress of superelastic reinforcement
e = eccentricity of the superelastic reinforcement

The nominal flexural strength thus calculated is equal to 15.8 KN.m. The capacity reduction factor times this nominal strength still exceeds the factored loads with the doubled live load (we have used the ACI load anc capacity reduction factors in this research; one may also use the AASHTO factors). Hence, the strengthened beam provides sufficient flexural strength for resisting the increased level of live load.

The nominal shear strength of the beam is 45.3 KN, which is sufficient for resisting the factored loads after doubling the live load applied on the beam.

The maximum crack width in the strengthened beam after doubling the live load is 0.2 mm which is comparable to the 0.19 mm crack width of the unstrengthened beam under the initial live load. The beam midspan deflection under full service load, after doubling the live load, is -0.25 mm (upward), which is quite reasonable noting that the unstrengthened beam exhibited 1.3 mm (downward) deflection under the initial service loads.

Repair and Strengthening with Shape-Memory Reinforcement

While the emphasis of this project is on superelastic reinforcement which provides self-repair capability, we also considered a shape-memory reinforcement which is not superelastic at ambient temperature for use in this project. This shape-memory reinforcement applies corrective prestressing forces through the constrained recovery phenomenon upon rise of temperature from below ambient to ambient level (after it has been plastically elongated at low temperature in the martensite phase).

The particular shape-memory reinforcement we used in this project was an iron-doped Ni-Ti with 55 % by weight Ni, 41.5% Ti, and 3.5% Fe. This shape-memory alloy provides a transformation (austenite finish) temperature of -120°C, and it is not superelastic at room temperature, which means that martensite can not be stress-induced at room temperature. The iron-doped Ni-Ti shape-memory alloy provides an austenite yield strength of 800 MPa and an elongation that exceeds 15%. The constrained recovery of this alloy, when it was elongated 3% in martensite phase at -180°C (in liquid nitrogen) and then allowed to warm up to room temperature in constrained condition, was 640 MPa. Hence, in order to apply the 55 KN corrective prestressing force required in our case, we used two 7.4-mm diameter rods of this alloy. The 3% prestrain allows us to fully utilize the constrained recovery potential of the alloy for the application of corrective forces. Also, the less than 0.2% long-term strain losses associated with concrete creep and

shrinkage and relaxation of the alloy do not cause any substantial loss of the prestressing forces due to the low unloading modulus of the shape-memory alloy (which is one of its unique advantages).

We analyzed the reinforced concrete beam which was repaired and strengthened with shape-memory alloy for serviceability and strength characteristics as we did in the case with superelastic alloy. The beam satisfied all the serviceability and strength requirements under twice the original live load after it was repaired.

Self-Repair with Superelastic Reinforcement

The superelastic reinforcement should be able to, upon the application and removal of overloads which cause yielding of reinforcing steel and excess crack opening in the reinforced concrete beam, apply corrective forces which cause compressive yielding in the reinforcing steel and closure of the cracks. This ability of the superelastic reinforcement

would allow for automatic restoration of the integrity and serviceability of the beam after it has been subjected to damaging overloads.

Noting that during accomplishing self-repair after the steel reinforcement has yielded the superelastic reinforcement applies the tress level (σ_{lower}) on its lower (unloading) plateau, the required area of the superelastic reinforcement (A_{sp}) for accomplishing the self-repair task described above is:

$$A_{sp} = A_s.f_y.(d-c_1^*)/[\sigma_{lower}(d_p-c_1^*)$$

The above equation, with the geometric attributes given in Figure 4, yields 124 mm^2 as the required area of the superelastic reinforcement. Fifty wires of 1.78 mm diameter provide this required area; the same number of wires also satisfied the repair and strengthening requirements. Hence, the repair/strengthening and the self-repair tasks can all be accomplished with the same number of superelastic wires. The superelastic reinforcement we have chosen can recover up to 8% strain through the superelasticity phenomenon. Noting that we subject the superelastic reinforcement to 3% initial prestrain, of which 0.6% would be lost for repair and short-term as well as long-term losses, it still provides 5.6% recoverable strain capacity to accomplish self-repair. This reserve strain capacity is quite large and can be used for self-repair after substantial cracking and deformation.

EXPERIMENTAL VERIFICATION OF THE TECHNOLOGY IN FLEXURE

Experimental Program

The reinforced concrete beams were first, before any strengthening and repair with shape-memory or superelastic reinforcement, subjected to three-point loading (Figure 25) until failure and into their post-peak region up to a maximum mid-span deflection of 12 mm when they were unloaded. This loading caused yielding of steel and excess opening of flexural cracks (Figure 26). The load-deflection curves were monitored during loading, and the crack widths were also measured.

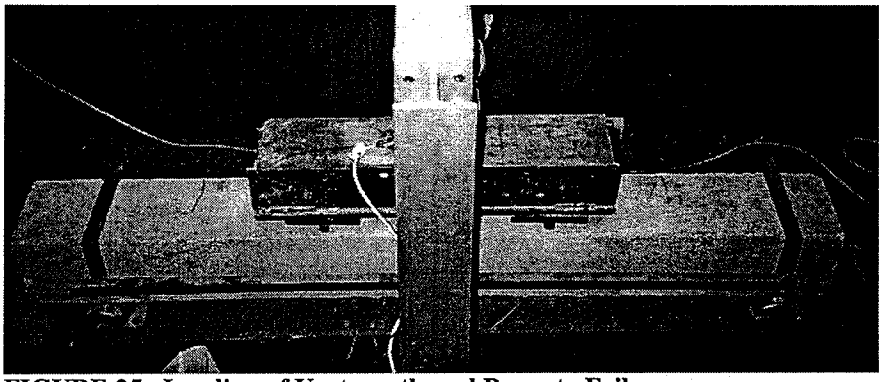

FIGURE 25. Loading of Unstrengthened Beam to Failure

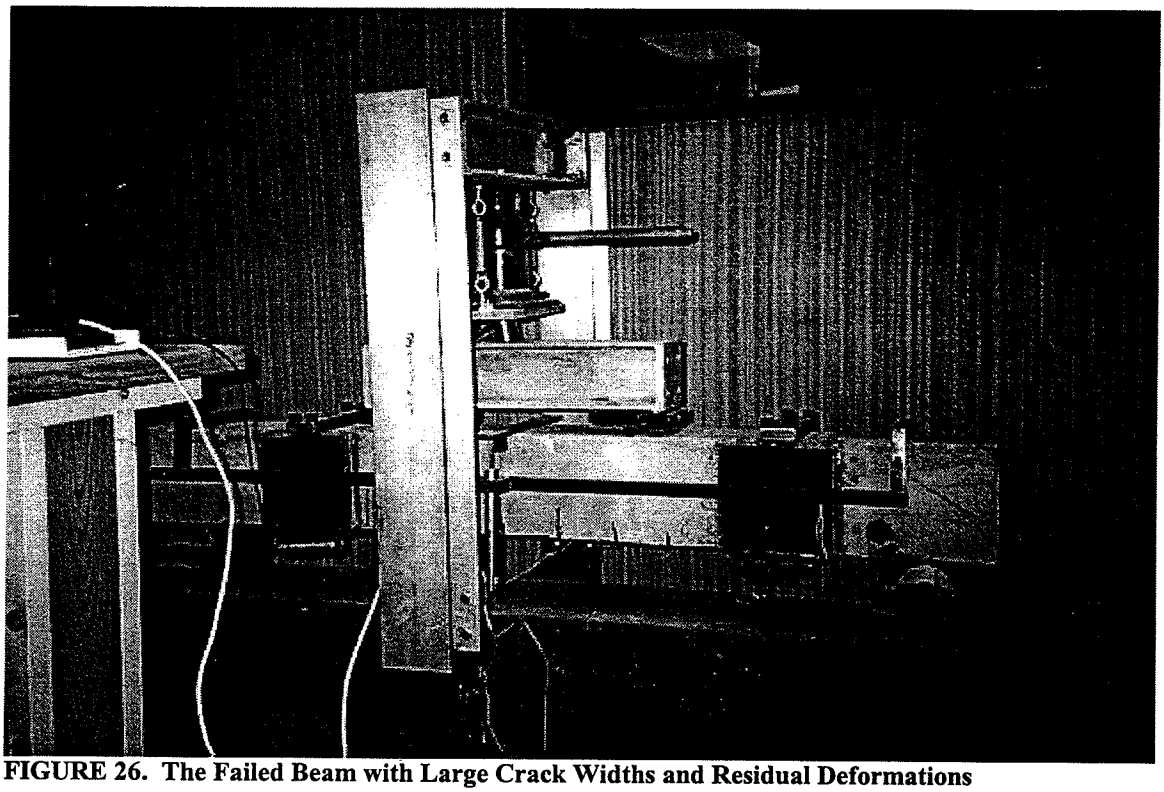

FIGURE 26. The Failed Beam with Large Crack Widths and Residual Deformations

The next step was to repair/strengthen the reinforced concrete beams with shape-memory or superelastic reinforcement. For this purpose, steel anchorages were adhered onto reinforced concrete beams using epoxy. The shape-memory and superelastic reinforcement were then subjected to liquid nitrogen and dry ice, respectively, for transition to martensite phase where they were subjected to a prestrain of 3%, unloaded (with the prestrain largely preserved), and attached to the end anchorages which were adhered onto the beam. Subsequently, as the shape-memory and superelastic reinforcement warmed up to ambient temperature, constraint of their shape recovery upon transformation to austenite by the beam transferred constrained recovery forces to the reinforced concrete beams which automatically accomplished the repair (crack closure and correction of deformations) and strengthening (post-tensioning) tasks without any additional work by the operator. Figure 27 shows the reinforced concrete beam repaired with the shape-memory reinforcement, and Figure 28 shows the beam repaired with superelastic reinforcement. The shape-memory rods which were available at larger diameters (7.4 mm) were threaded and connected to the anchorage system using bolts. End anchorage of the smaller superelastic wires (1.78 mm diameter) involved embedding their ends into an aluminum plate cast around them. We measured mid-span deflection and crack widths as the shape-memory or superelastic reinforcement warmed up to ambient temperature and accomplished the repair and strengthening (post-tensioning) tasks.

FIGURE 27. The Beam Repaired/Strengthened with Shape-Memory Reinforcement

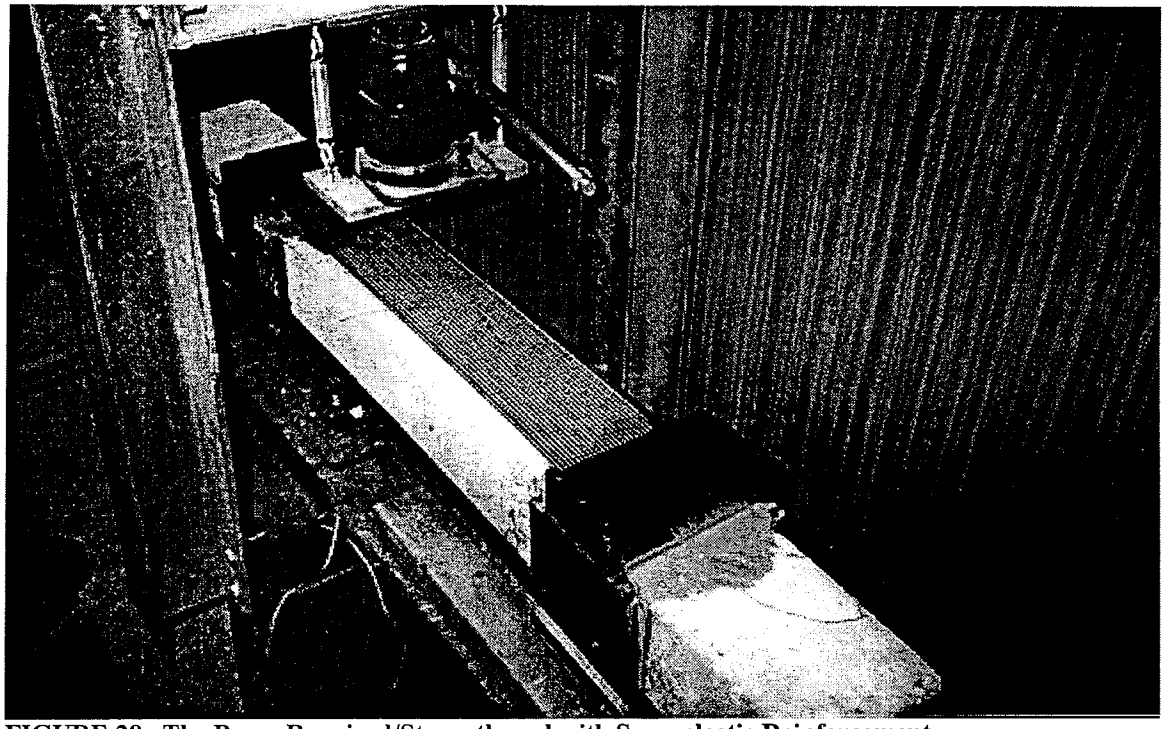

FIGURE 28. The Beam Repaired/Strengthened with Superelastic Reinforcement

After the above repair/strengthening steps, the beams were again subjected to third-point loading (Figures 29 and 30) up to the original service load and then the increased service load (with live load doubled), and the load-deflection relationships as well as crack widths monitored in the process. In the case of the reinforced concrete beam repaired/strengthened with superelastic reinforcement, we also verified the self-repair capability by loading the beam to failure; we then observed the closure of cracks and correction of post-yield deformations after the system automatically accomplished self-repair upon unloading.

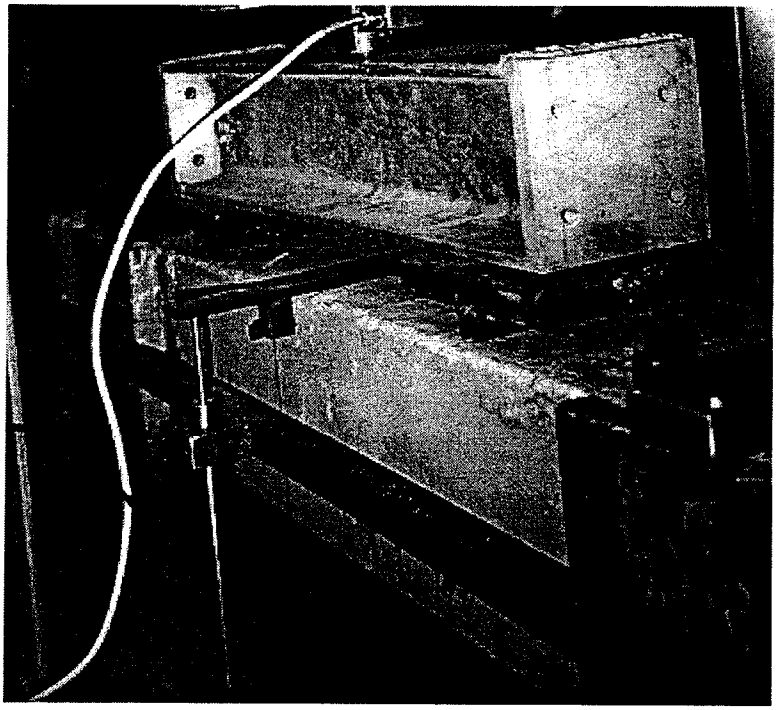

FIGURE 29. Loading of the Beam Repaired/Strengthened with Shape-Memory Reinforcement

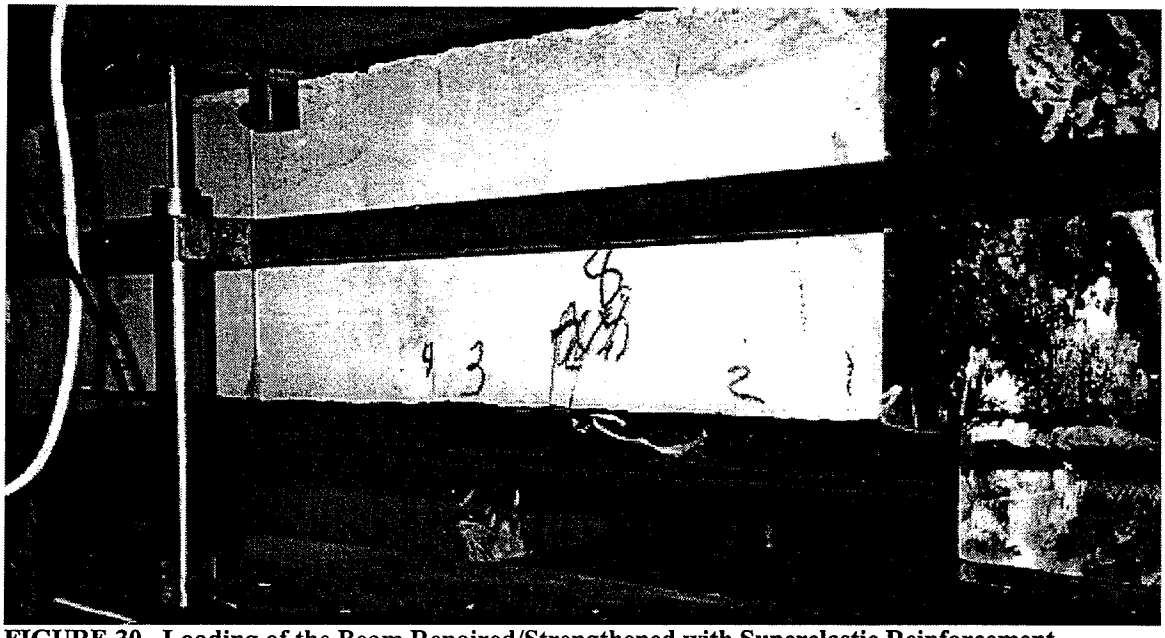

FIGURE 30. Loading of the Beam Repaired/Strengthened with Superelastic Reinforcement

Test Results

The load-deflection curves for beams loaded to failure and then repaired/strengthened with shape-memory and superelastic reinforcement are presented in Figures 31 and 32, respectively. Loading of the repaired beams beyond their elastic limit will be discussed later in this section. These curves confirm that warming up of the shape-memory and superelastic reinforcement to ambient temperature corrects the residual deformations after initial loading to failure. This process also practically closed all the cracks opened after initial post-yield loading; the crack widths reduced from about 1.4 mm in failed beams to less than 0.1 mm in repaired beams. Repair and strengthening with both shape-memory and superelastic reinforcement enhanced the serviceability of beams and, as is observed in the post-repair segments of the load-deflection curves in Figures 31 and 32, led to a satisfactory behavior under live loads twice as large as the initial loads. At this increased load level the mid-span deflection was less then 0.002 times the span length and the maximum crack widths were less than 0.2 mm. Both deflections and crack widths were fully recovered upon unloading. This confirms that the tasks of repair and strengthening were successfully accomplished with both the shape-memory and the superelastic reinforcement. The superelastic reinforcement also provides the unique feature of self-repair, to be discussed in the following.

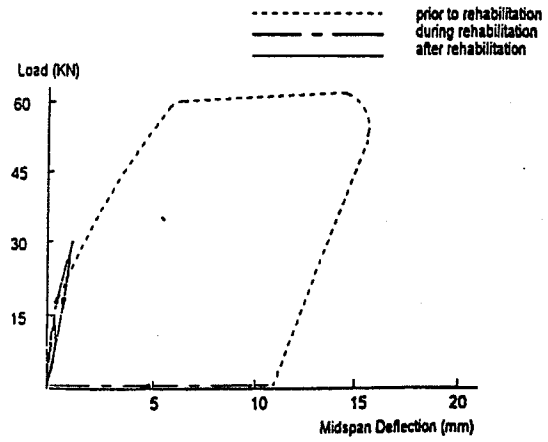

FIGURE 31. Experimental Load-Deflection Behavior of the Beam Strengthened with Shape-Memory Reinforcement

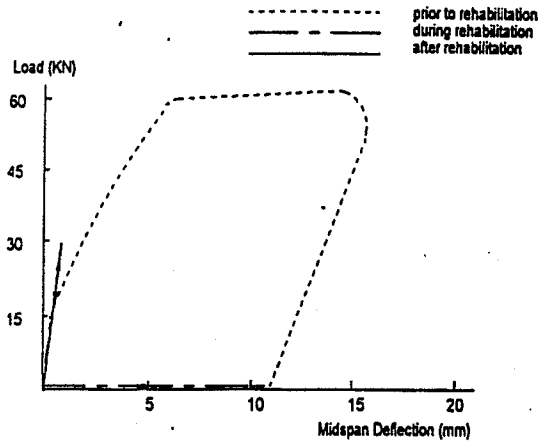

FIGURE 32. Experimental Load-Deflection Behavior of the Beam Strengthened with Superelastic Reinforcement

The load-deflection relationships of the original and rehabilitated beam after loading to about 15 mm midspan deflection followed by unloading are presented in Figure 33. The superelastic reinforcement system is observed to successfully accomplish the following objectives: (1) the load carrying capacity of the beam is increased from 60 KN to 100 KN; and (2) the superelastic reinforced beam provides an inherent self-repair capability upon load removal, and thus no permanent deformations remain after unloading; and (3) the opening of cracks in the beam repaired with superelastic reinforcement occurs at a load of 45 KN as compared with the 20 KN first crack load of the original beam. During loading of the superelastic reinforced beam to 15 mm midspan deflection, we also monitored the opening of cracks. The cracks that opened during initial loading of the unstrengthened beams opened again in the process, reaching a maximum width of 0.6 mm (Figure 34a); upon load removal, however, the self-repairing action of the superelastic reinforcement caused practically full closure of the cracks (Figure 34b).

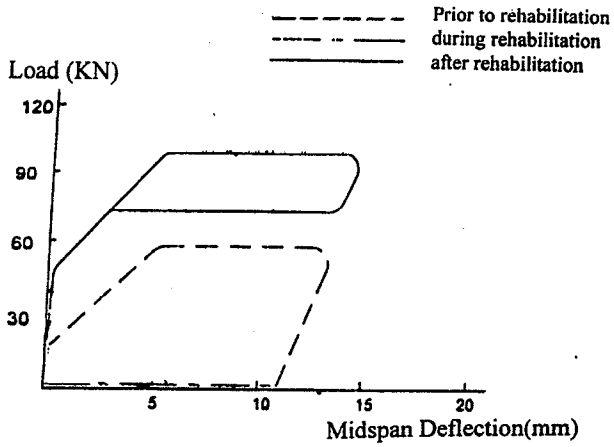

FIGURE 33. Self-Repair in Superelastic Reinforced Beam

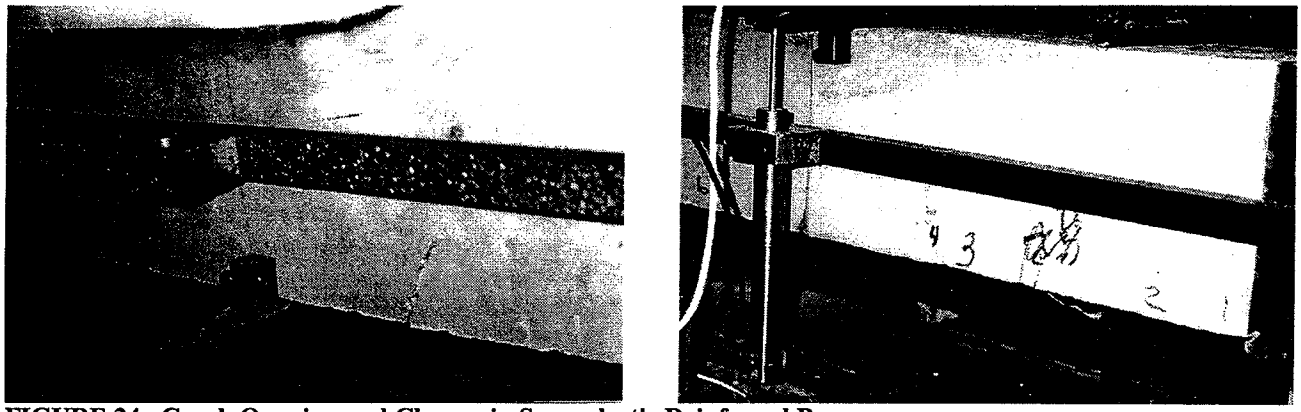

FIGURE 34. Crack Opening and Closure in Superelastic Reinforced Beam

VERIFICATION OF THE TECHNOLOGY USING SUPERELASTIC FIBER COMPOSITE

The use of composite sheets for the rehabilitation of reinforced concrete bridges and other structures has been gaining popularity in the recent years. These sheets can be conveniently adhered onto the structural elements to accomplish strengthening effects. Superelastic reinforcement is available in fine diameters suiting embedment in thin polymer composites. In the context of our application (Figure 35), the polymer matrix composite provides end bonding surfaces to concrete while a free (unadhered) middle part of the system provides the rehabilitating and self-repairing effects we are seeking in our application.

A carbon fiber reinforced epoxy in the form of prepreg laminate (5245C prepreg system manufactured by CYTEC Engineering Materials, Inc. of Anaheim, California) was used to build the superelastic fiber reinforced polymer matrix composite. Superelastic fibers of 0.2 mm diameter were sandwiched between 5 prepreg laminates on each side, with laminates placed in perpendicular directions in subsequent layers. The composite system was then cured and post-cured under vacuum while applying mechanical pressure and high temperature (Figure 36) following manufacturer's recommendation. The composite incorporated a superelastic reinforcement volume fraction of 22%, which comprised 180 fibers of 0.2 mm diameter placed over a width of 60 mm in the composite.

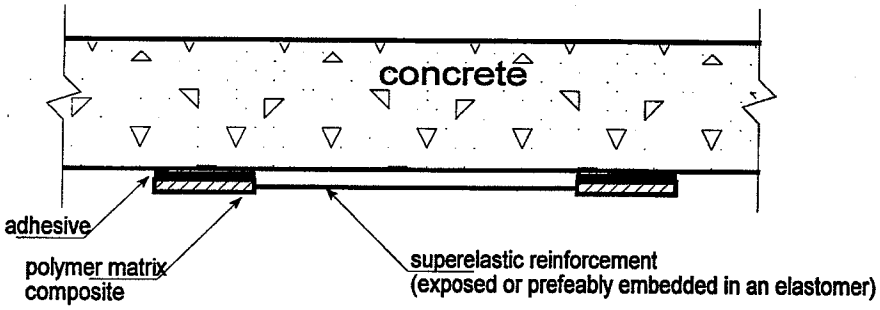

FIGURE 35. Repair with Superelastic Fiber Reinforced Composite System

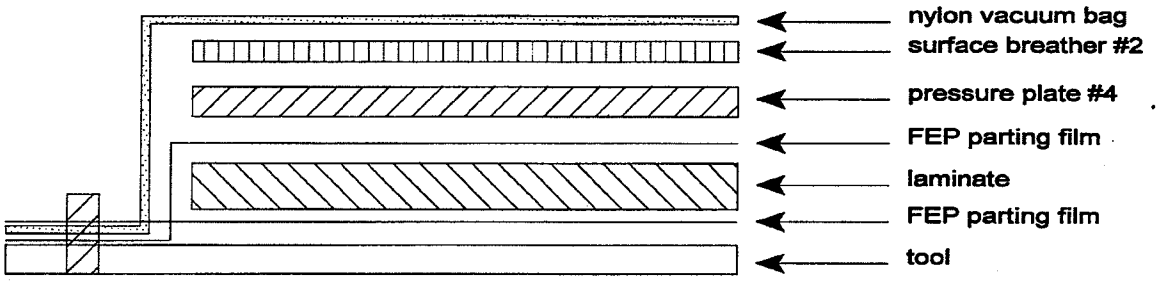

FIGURE 36. The Curing Set-Up for Polymer Matrix Composite

We used a steel fiber reinforced concrete with 1% volume fraction of steel fibers of 0.45 mm diameter and 31 mm length to demonstrate the self-repairing capabilities rendered by the new composite system to structures. While this particular experiment used steel fibers, one could also use conventional reinforcement steel in this test. The fiber reinforced concrete specimen strengthened by superelastic fiber reinforced polymer matrix composite is shown in Figure 37a. The weakened area of this tensile specimen provides a cross-sectional area of 1,500 mm^2; this area after it has cracked (according to our background tests) requires a crack closure force of 4,500 N (or a crack closure pressure of 3 MPa). We would need a total of 360 wires (180 on each side) to provide self-repairing (crack closing) capability for this system (see Figure 37b). The strengthened system shown in Figure 37b was not prestressed. Prestressing would have been required if the specimen was cracked and superelastic reinforcement had to repair the specimen in addition to strengthening it. Epoxy adhesive (manufactured by Ad-Tech) was used to adhere the polymer composites to concrete surfaces. Figure 38 presents a picture of the strengthened specimen which was subjected to tensile loading and unloading.

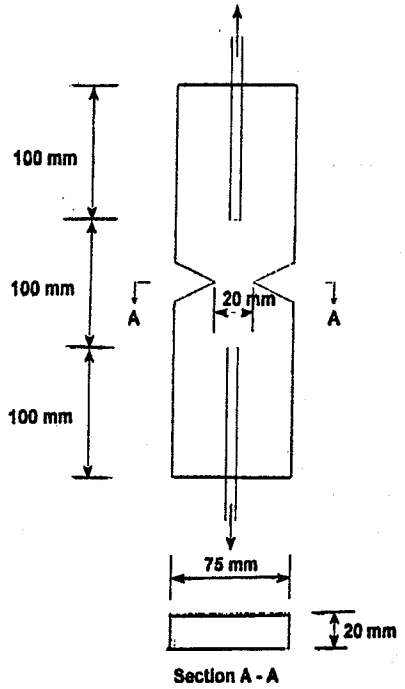

(a) Unstrengthened Specimen

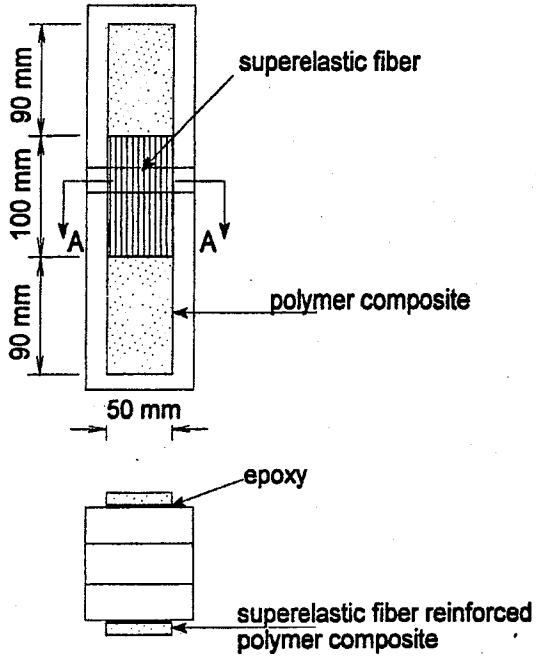

(b) Strengthened Specimen

FIGURE 37. Tensile Specimen Before and After Strengthening with Polymer Composite

FIGURE 38. Picture of the Concrete Specimen Strengthened with Polymer Composite

Figure 39 presents the test results after tensile loading and unloading of unstrengthened and strengthened concrete specimens of Figure 37. The superelastic reinforced composite is observed to successfully accomplish the task of self-repair after a crack opening exceeding 3 mm. These cracks were reduced to hairline cracks after unloading. These results confirm that superelastic fiber reinforced composites can conveniently strengthen concrete structures and provide them with self-repair capability.

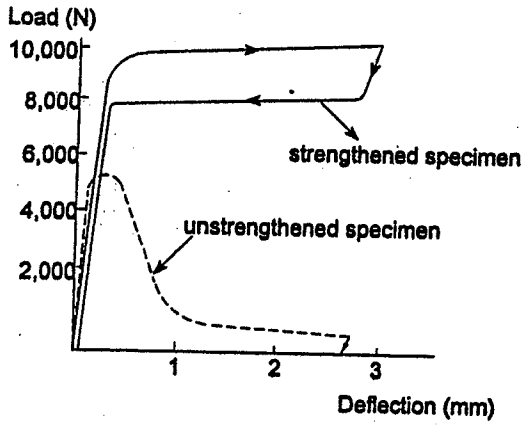

FIGURE 39. Tension Test Results

COST ANALYSIS

Our technology provides an expedient, efficient, low-cost and simple approach with unique damage control and self-repair features for repair and strengthening of structural systems. In order to demonstrate the advantages of the technology in terms of cost and time savings, we used a reinforced concrete bridge pier cap in Michigan which requires strengthening due to deficient design procedures. More specifically, the structural system lacks sufficient shear strength near end supports. Michigan Department of Transportation has chosen a strengthening technique involving post-tensioning with steel cables (Figure 40). The total cost of this approach to strengthening of four pier caps in this bridge add up to $740,000. The total cost here covers the material, labor, equipment and engineering expenses as well as the cost implications of bridge closure. This conventional approach can be completed in three weeks, and requires the bridge to be closed for 126 hours.

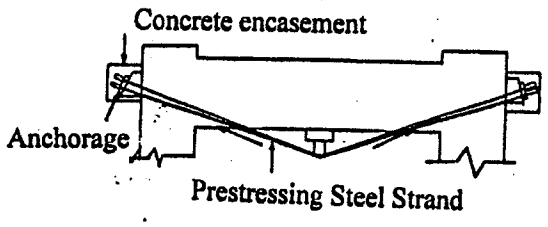

FIGURE 40. Conventional Bridge Pier Cap Strengthening

The alternative superelasticity-based approach to strengthening of this bridge (Figure 41) involves local post-tensioning using superelastic rods and epoxy-bonded anchorages. The practical immunity of superelastic reinforcement to the loss of prestressing forces allows local post-tensioning over short lengths and the use of convenient epoxy-bonded anchorages. The superelasticity-based strengthening system also provides unique safety features of self-repair and damage control (high distributed energy absorption) which would be missing in the conventional approach. The total estimated cost of this alternative superelasticity-based approach added up to $435,000 and the estimated duration of work was reduced to five days, with only 30 hours of bridge closure. The bulk of savings resulted from the reduced spending at the job site on labor and anchorages, and also from the reduced duration of bridge closure. The cost break-down of the conventional approach was as follows: 20% materials, 10% engineering and labor, 10% equipment, and 60% bridge closure. In the case of the superelasticity-based approach, the cost break-down was as follows: 35% materials, 17% engineering and labor, 18% equipment, and 30% bridge closure. Savings in cost and time when added to the substantially improved safety and reliability obtained with the new system make the superelasticity-based approach clearly advantageous in this application.

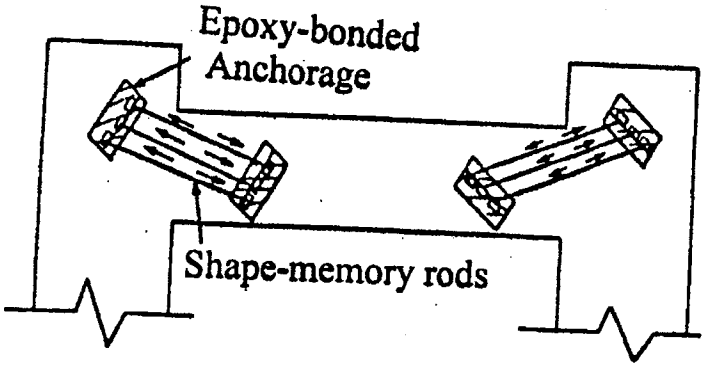

FIGURE 41. Superelasticity-Based Bridge Pier Cap Strengthening

SUMMARY AND CONCLUSIONS

The main goal of our project was to determine the technical feasibility and economic viability of the superelasticity-based approach to repair and strengthening of bridge structures. The new system also provides structural systems with unique features for damage control and self-repair. Our project successfully accomplished its goal; a brief summary of the project and its key findings are summarized below.

1. A superelastic alloy, Ni-Ti-Cr, was selected to provide high levels of recoverable strain, recovery stress, strain capacity, and ultimate strength. The processing conditions of this alloy were optimized for use in this investigation.

2. The selected superelastic alloy was subjected to a comprehensive experimental investigation. The alloy exhibited excellent performance characteristics in terms of relaxation resistance under sustained loads, stability under cyclic loads, corrosion resistance, stable behavior at different temperatures, and high recoverable strain, recovery stress, ultimate strength and elongation and energy absorption capacity.

3. Structural design procedures were developed for repair and strengthening of reinforced concrete systems through post-tensioning with superelastic-based systems. These design procedures cover the repair (crack closure and deflection recovery), strengthening (capacity and serviceability enhancement), and self-repair aspects of the technology.

4. The technology was experimentally verified in two applications. One application tested the repair, strengthening and self-repair features of the technology using a reinforced concrete beam which had experienced excess cracking and inelastic deformations under load. Post-tensioning with superelastic rods proved to be a highly effective approach for the repair of this beam and for strengthening it to resist higher service and ultimate load levels; this system also provided the repaired and strengthened beam with a unique self-repair capability when subjected to severe loads. The second application used epoxy-bonded superelastic fiber reinforced composite sheets to strengthen a concrete component and provide it with self-repair capability. The test results verified that the superelastic-based composite successfully achieved the strengthening and self-repair objectives in this application.

5. We assessed the cost and time savings associated with the use of our technology in a typical application involving strengthening of a reinforced concrete bridge pier cap which was deficient in shear strength. Our technology was compared in this application with a conventional prestressing approach using steel strands. The superelasticity-based system, when compared with the conventional approach, yielded 40% cost saving and 75% reduction in the required bridge closure duration.

In conclusion, the superelasticity-based rehabilitation technology developed and verified in this research offers an expedient, low-cost and highly reliable approach to structural repair and strengthening. The superelasticity-based system provides unique features for damage control and self-repair under severe loading conditions. The practical immunity of the superelastic prestressing system to the losses of prestressing force broadens the selection of convenient, rapid and low-cost anchorages. The high corrosion resistance of superelastic alloys also ensures desirable durability of the new repair and strengthening system.

REFERENCES

1. Wayman, C.M. and Duerig, T.W., "An Introduction to Martensite and Shape Memory," Engineering Aspects of Shape Memory Alloys (T.W. Duerig, K.N. Melton, D. Stockel and C.M. Wayman, editors), Butterworth-Heinmann, Boston, MA, 1990, pp. 3-21.

2. Duerig, T.W. and Zadno, R., "An Engineer's Perspective of Superelasticity," Engineering Aspects of Shape Memory Alloys (T.W. Duerig, K.N. Melton, D. Stockel and C.M. Wayman, editors), Butterworth-Heinmann, Boston, MA, 190, pp. 369-393.

3. Stockel, D. and Yu, W., "Superelastic Ni-Ti Wire," Proceedings, 60th Annual Convention and 1990 Division Meeting of the Wire Associate International, Inc., Boston, MA, Oct. 1990, pp. 172-177.

4. Nilson, A.H., "Design of Prestressed Concrete," John Wiley & Sons, 1978, pp. 107-111.